

Priority Aware Frame Packing for OFDMA Systems in Distributed Permutation Mode

Keivan Bahmani

Submitted to the
Institute of Graduate Studies and Research
in partial fulfillment of the requirements for the Degree of

Master of Science
in
Electrical and Electronic Engineering

Eastern Mediterranean University
June 2013
Gazimağusa, North Cyprus

Approval of the Institute of Graduate Studies and Research

Prof. Dr. Elvan Yılmaz
Director

I certify that this thesis satisfies the requirements as a thesis for the degree of Master of Science in Electrical and Electronic Engineering.

Prof. Dr. Aykut Hocann
Chair, Department of Electrical
and Electronic Engineering

We certify that we have read this thesis and that in our opinion, it is fully adequate, in scope and quality, as a thesis of the degree of Master of Science in Electrical and Electronic Engineering.

Assoc. Prof. Dr. Erhan A. İnce
Supervisor

Examining Committee

1. Prof. Dr. Aykut Hocann

2. Assoc. Prof. Dr. Erhan A. İnce

3. Assoc. Prof. Dr. Dođu Arifler

ABSTRACT

As of today the two candidates for 4G which has been commercially deployed are the Institute of Electrical and Electronics Engineers (IEEE) standard 802.16e (“Mobile WiMaX”) and the 3rd Generation Partnership Project (3GPP) standard Long Term Evolution (LTE-Advanced).

Both standards make use of Orthogonal Frequency Division Multiple Access (OFDMA) as their downlink modulation schemes and allocations for users must be carried out using both time and frequency (sub-channels vs. symbols). In this thesis we focus on the IEEE 802.16e in Partially Used Sub-Carrier (PUSC) mode which is taking advantage of frequency diversity. For each 5 milliseconds frame, the data for different users must be placed into the DL part of the frame based on the decision of a scheduler. Once the scheduling is complete a packing algorithm will then try to fit all requests into the frame considering channel quality, selecting Modulation and Coding Scheme (MCS) and deciding on the number of bytes per slot per burst.

The empirical channel model adopted in the thesis is the COST 231 extended version of the Hata model using 2360-2370 MHz band. All simulations were done using the MATLAB platform and writing dedicated functions for each task. We consider an urban microcell environment and assume that based on the traffic characteristics the admission control module has admitted 20 connections. The cell coverage area was assumed to be circular with a diameter of 4 km. The starting values of the radial distance (in meters) of the mobile stations in the cell were determined using varieties drawn from a uniform distribution in the range 100-2000 meters. Then, for the future

frames, the position of each Mobile Station (MS) was re-calculated assuming a vehicular speed chosen uniformly between 0-60 km/h either towards or away from the Base Station (BS).

First, the well-known Enhanced One Column Stripping with Non-Increasing Area First Mapping (eOCSA) algorithm was used for packing and then a novel packing algorithm making use of priority aware packing was proposed to extend the eOCSA in order to get a more efficient packing algorithm. In the priority-aware extended eOCSA algorithm each user was given a priority number between 1 and 6. When the number is 1 or 2, the user's bursts are assumed to be "low-priority", and when it is between 3 and 6, the bursts are considered to be "high-priority." The priority-aware packing algorithm would first pack the bursts in the high-priority class and then would move on to the ones in the low-priority class. If a burst cannot be fitted into a frame, its priority number would be increased (by one unit) in an attempt to upgrade its class in the next frame. That way, the leftover bursts would be progressively given higher priority numbers in upcoming frames. If the priority number associated with a burst become larger than 6, the algorithm would drop that burst. To show the effectiveness of the newly proposed priority aware packing algorithm we compared the average percentage of unallocated burst in our proposed algorithm against that of eOCSA which was obtained using 6 seconds worth of simulation (1200 frames) for the 100 times the simulation was repeated.

Keywords: SOFDMA; WiMaX; PUSC; eOCSA; Priority-Aware eOCSA

ÖZ

4G'nin ticari olarak işleme konan iki adayı Elektrik ve Elektronik Mühendisleri Enstitüsü (IEEE) standardı 802.16e (mobil WiMaX) ve 3. Nesil Ortaklık Projesi (3GPP) standardı Uzun Süreli Evrim dir (LTE-İleri Düzey). Bu standartların ikisi de aşağı bağlantı kiplemesi olarak Dikgen Frekans Bölmeli Çoklu Erişimini (OFDMA) kullanmakta ve özgülleme hem zaman hem de frekansda (alt kanallara karşı semboller) yapılmaktadır. Bu tez, frekans çeşitliliğini avantaj olarak kullanan Kısmi Kullanılmış Alt Taşıyıcı (PUSC) modundaki IEEE 802.16e üzerinde yoğunlaşmaktadır. Farklı kullanıcılara ait veriler çizelgeleyicinin kararına göre beş mili saniye aralarla olan çerçevelerin aşağı bağlantı bölümüne yerleştirilmelidir. Çizelgeleme sona erdikten sonra, bir yerleştirme algoritması kanal kalitesini göz önünde bulundurarak, Modülasyon Kodlama Düzenini (MCS) seçerek ve dilim başına düşen bayt sayısını belirleyerek bütün istekleri çerçeveye sığdırmaya çalışacaktır.

Bu tezde kullanılan ampirik kanal modeli, 2360-2370 MHz bandını kullanan Hata modelinin geliştirilmiş bir versiyonu olan COST 231'dir. Tüm benzetimler MATLAB platformunu kullanarak ve her görev için özel fonksiyonlar yazarak gerçekleştirilmiştir. Benzetimler kentsel makrohücre ortamı ve 20 kullanıcı varsayımı ile elde edilmiştir. Hücre kapsama alanının 4 km çapında ve dairesel olduğu varsayılmış ve düzgün dağılımdan elde edilen rastgele değerlerle (100-2000 metre arası bir değer alacak şekilde) hücredeki mobil istasyonların radyal mesafeleri belirlenmiştir. Daha sonra, gelecekteki çerçeveler için her Mobil İstasyonun (MS)

pozisyonu taşıt hızı Baz İstasyonundan (BS) yada Baz İstasyonuna doğru saatte 0-60 km olarak tahmin edilerek yeniden hesaplanmıştır.

İlk olarak, yoğunlaşma sağlamak için iyi bilinen eOCSA algoritması kullanılmış ve daha sonra de daha etkin bir yoğunlaşma sağlayacak ve önceliklerin farkında olan eOCSAın geliştirilmiş bir versiyonu önerilmiştir. Başlangıçta önceliklerin farkında olan genişletilmiş eOCSA algoritması her kullanıcıya 1 ve 6 arasında bir öncelik sayısı vermiştir. Bu sayı 1 veya 2 olduğunda kullanıcıların önceliğinin "düşük "; 3 ve 6 arasında olduğunda ise "yüksek" olduğu varsayılmıştır. Öncelik-farkındalığı olan algoritma ilk olarak yüksek öncelikli patlamaları yoğunlaştırmaya başlamakta ve daha sonra düşük öncelikleri olanlara geçmektedir. Bir patlamanın çerçeveye yerleştirilememsi durumunda bir sonraki çerçevede sınıfının yükseltilmesi amacı ile bu patlamaların öncelik sayısı bir birim artırılmıştır. Bu sayede, artık patlamalara bir sonraki çerçeveler için kademeli olarak daha yüksek öncelik numaraları verilmektedir. Bir patlama için verilen öncelik sayısı 6'yı aştığında ise bu patlama düşürülmektedir. Yeni önerilen ve öncelik farkındalığı olan algoritmanın etkinliğini göstermek amaçlı 100 kez tekrarlanan 6 saniyelik (1200 çerçeve) benzetimler gerçekleştirilmiş ve elde edilen sonuçlar ve eOCSA için patlamaları yoğunlaştıramama avaraj yüzdeler değeri karşılaştırılmıştır.

Anahtar kelimeler: SOFDMA; WiMaX; PUSC; eOCSA; Priority-Aware eOCSA

Dedicated to

my mother Zahra Keshavarz and my sister Katayoun Bahmani
who have always been supportive of me during my time at EMU.

ACKNOWLEDGMENTS

First and foremost I would like to thank my supervisor Assoc. Prof. Dr. Erhan A. İnce for guiding and helping me in my master study, for his patience and sharing kindly his knowledge with me.

Besides my supervisor, I would also like to thank Assoc. Prof. Dr. Doğu Arifler for his collaboration with us on some publications we have done together.

I also wish to thank all the faculty members at the department of Electrical and Electronic Engineering, and specially the chairman, Prof. Dr. Aykut Hocann.

Last but not least, I would like to express my appreciation to my parents and my sister who has always given me support and encouragement.

TABLE OF CONTENTS

ABSTRACT	iii
ÖZ.....	v
DEDICATION	vii
ACKNOWLEDGMENTS	viii
LIST OF FIGURES	xi
LIST OF TABLES	xiii
LIST OF SYMBOLS AND ABBREVIATIONS	xiv
1 INTRODUCTION.....	1
1.1 Background.....	6
1.2 Thesis Description	8
1.3 Thesis Contributions.....	9
2 OFDM, OFDMA AND SOFDMA.....	11
2.1 FDM	11
2.2 OFDM.....	13
2.2.1 DFT and IDFT and FFT.....	15
2.2.2 Cyclic Prefix.....	16
2.3 OFDMA And SOFDMA	18
2.3.1 Sub-channelization.....	20
3 DL-PUSC: A DISTRIBUTED PERMUTATION MODE FOR WIMAX	23
3.1 Downlink PUSC	23

3.2	MATLAB GUI	30
4	COST-231 HATA Channel MODEL FOR IEEE 802.16E.....	32
4.1	COST-231 Hata Model Path Loss	32
4.2	Macro Cell Urban Environment	34
4.3	Modulation and Coding Scheme (MCS) In IEEE 802.16e	36
5	FRAME PACKING ALGORITHMS	38
5.1	OCSA	39
5.2	eOCSA.....	41
5.3	Orientation Based Burst Packing (OBBP)	44
5.4	Versions of the Proposed Algorithm	44
5.4.1	Extended eOCSA with Regular Plus the Leftover Bursts	45
5.4.2	Priority-Aware Extended eOCSA	45
6	PERFORMANCE ANALYSIS FOR PACKING ALGORITHMS	48
7	CONCLUSIONS AND FUTURE WORK	59
7.1	Conclusions	59
7.2	Future Work.....	60
8	REFERENCES	61

LIST OF FIGURES

Figure 1.1: WIMAX Frame.....	4
Figure 2.1: Spectrum of FDM.....	11
Figure 2.2: FDM Modulation.....	13
Figure 2.3: FDM Demodulation.....	13
Figure 2.4: Five Sub-carrier OFDM System.....	14
Figure 2.5: OFDM System Diagram.....	15
Figure 2.6: Effect of ISI on Symbols.....	16
Figure 2.7: Deep Fades in The Frequency Response.....	17
Figure 2.8: Cyclic Prefix in Time Domain.....	18
Figure 2.9: Example of OFDMA.....	19
Figure 2.10: Example of Using Segmentation with Frequency Reuse Factor N=1 ...	22
Figure 3.1: Sub-carriers in The 1024 FFT.....	24
Figure 3.2: Absolute Sub-carrier Indices of Sub-carriers in ‘PermBase 0’.....	26
Figure 3.3: Pilot Sub-carriers of Logical Cluster 0.....	27
Figure 3.4: Absolute Sub-carrier Indices for Sub-carriers of ‘Sub-channel 0’.....	29
Figure 3.5: GUI for PUSC-DL Calculations.....	30
Figure 3.6: GUI Showing The Absolute Subcarrier Indices for Subcarrier 5 of Sub- channel 3 for an ODD OFDM Symbol.....	31
Figure 4.1: Path Loss Calculated With COS-231 Hata Model.....	34
Figure 4.2: SNR for Different Distances.....	35
Figure 5.1: Example of Frame Packed Using OCSA.....	41
Figure 5.2: Example of Frame Packed Using eOCSA.....	43

Figure 5.3: Examples of Downlink Part of the Frame Packed With Proposed Algorithm.....	47
Figure 6.1: Distance of MS From Base Station in Occasion1	49
Figure 6.2: Distance of MS From Base Station in Occasion2	50
Figure 6.3: Location of MS #1 During One Simulation Run.....	50
Figure 6.4: Location of MS #2 During The Same Simulation Run as in Fig. 6.3	51
Figure 6.5: Distance of Users From Base Station	51
Figure 6.6: Path Loss for Individual Users in The Frame	52
Figure 6.7: SNR of Each User in The Frame	52
Figure 6.8: Frame Packed Using eOCSA.....	53
Figure 6.9: Frame Packed Using Extended eOCSA	54
Figure 6.10: Percentage of Unallocated Bursts for eOCSA in 100 Trials	54
Figure 6.11: Percentage of Unallocated Bursts Using Extended eOCSA for 100 Trials	55
Figure 6.12: Percentage of Unallocated Bursts Using Priority-Aware Extended eOCSA Under Normal Load for 100 Trials	56
Figure 6.13: Percentage of Unallocated Bursts Using Priority Aware Extended eOCSA Under 20% Extra Load for 100 Trials.....	57
Figure 6.14 : Percentage of Unallocated Bursts Using eOCSA Under 20% Extra Load for 100 Trials	58

LIST OF TABLES

Table 2.1: SOFDMA Parameter For “Mobile WiMaX”	20
Table 3.1: Major Groups and Their Sub-channels	27
Table 3.2: Absolute Sub-carrier Indices of ‘Sub-channel 0’	29
Table 4.1: Parameter Used in Simulation.....	34
Table 4.2: Burst Profiles from IEEE 802.16-2004.....	37
Table 4.3: DL Byte/Slot for “Mobile WiMaX” in PUSC Mode.	37
Table 5.1: Width and Height Pairs Calculated By OCSA for $\{A_i\} = 40$	39
Table 5.2: Width and Height Pairs Calculated By OCSA for $\{A_i\} = 37$	40

LIST OF SYMBOLS AND ABBREVIATIONS

A_i	Area of the burst
B_{coh}	Coherence bandwidth of the channel
c_m	Correction parameter
E_0	Initial offset parameter
E_{sys}	Initial system design parameter
f	Frequency
G	Ratio of T_G to T_d
G_R	Gain of the receiver
G_T	Gain of the transmitter
H_0	Maximum available height
H_i	Height of the burst
k	Sub-carriers index
N	Number of samples
N	Noise power at the receiver
N_c	Number of sub-carriers
N_{cp}	Number of sub-carriers in cyclic prefix
N_{fft}	Number of FFT points
P/s	Parallel to serial convertor
$P_s[.]$	Permutation sequence
P_T	Transmission power of base station
PL	Path loss
R	Baud Rate

$R_{(t)}$	Received signal
S	Sub-channel
$s(n)$	OFDM symbol
T_{coh}	Coherence time of the channel
T_s	Symbol duration
T_d	useful length of symbol
T_G	length of cyclic prefix in symbol
W	Bandwidth of the channel
W_i	Width of the burst
x	Input of the modulator
y	Output of the demodulator
β_{sys}	Slope of the model curve
Δf	Sub-carrier spacing
τ_{max}	Maximum excess delay
μs	Microsecond
16QAM	16 level Quadrature Amplitude Modulation
64QAM	64 level Quadrature Amplitude Modulation
AR	Autoregressive
AWGN	Additive Whit Gaussian Noise
AMC	Adaptive Modulation and Coding
AAS	Adaptive Antenna System
BER	Bit Error Rate
BF	Best Fit algorithm
BPSK	Binary Phase Shift Keying
BS	Base Station

dB _i	decibel isotropic
dBW	decibel Watt
DC	Direct current
DFT	Discrete Fourier Transform
DIUC	Downlink Interval Usage Code
DL	Downlink
DL-MAP	Downlink MAP
DL-PermBase	Downlink Permutation base
DSP	Digital Signal Processing
eOCSA	Enhanced One Column Striping with non-increasing Area first mapping
FDM	Frequency Division Multiplexing
FFT	Fast Fourier Transform
FUSC	Full Usage of Sub-channels
FCH	Frame Control Header
Gbps	Giga bit per second
GHz	Giga Hertz
GUI	Graphical User Interface
IEEE	Institute of Electrical and Electronics Engineers
IP	Internet Protocol
ISI	Inter Symbol Interference
ITU	International Telecommunication Union
km/h	Kilometer per Hour
LTE	Long Term Evolution
MB	Mega Bit

MCS	Modulation and Coding Scheme
MIMO	Multiple Input Multiple Output
MS	Mobile Station
ms	Milliseconds
MWA	Mobile Web Access
OBBP	Orientation Based Burst Packing
OCSA	One Column Striping with non-increasing Area first mapping
OF	Orientation Factor
OFDM	Orthogonal Frequency Division Multiplexing
OFDMA	Orthogonal Frequency Division Multiple Access
SOFDMA	Scalable Orthogonal Frequency Division Multiple Access
PUSC	Partially Usage of Sub-channels
PUSC DL	Partially Usage of Sub-channels in Downlink
QAM	Quadrature Amplitude Modulation
QoS	Quality of Service
RF	Radio Frequency
RTG	Receive Transition Gap
SINR	Signal to Interference and Noise Ratio
SNR	Signal to Noise Ratio
SNR_{loss}	Signal to noise ratio loss because of cyclic prefix
STBC	Space Time Block Code
TTG	Transmit Transition Gap
UIUC	Uplink Interval Usage Code
VBR	Variable Bit Rate
VOIP	Voice over Internet Protocol

WI-FI	Wireless Fidelity
WIMAX	Worldwide Interoperability for Microwave Access
WLFF	Weighted Less Flexibility First

Chapter 1

INTRODUCTION

With the ever increasing demand for wireless communication of multimedia traffic, broadband wireless networks are becoming increasingly important for our decade. However when the channel is a wideband channel special attention is required to deal with the fluctuations in the frequency response of a channel which are due to multipath propagation. 4G systems mostly are designed using MIMO-OFDMA and since OFDM can divide a broadband channel into multiple narrowband channels they can mitigate the effect of multipath propagation and also provide better link reliability.

4G which is also referred to as "Beyond 3G", is a fourth generation technology for wireless communication networks. The main idea behind 4G is convergence. It tries to provide interoperability between wired and wireless networks, wireless technologies including GSM, wireless LANs, Bluetooth as well as computers. Deployment of 4G networks had started in 2010 and is expected to continue beyond 2015.

4G is being developed as an all IP system that will provide 100 Mbps for users with high mobility and 1 Gbps for users that are moving at a slower speed. Beside the increase in data rate it aims to provide an end-to-end QoS and improved security.

International Telecommunications Union (ITU) has specified the IMT-Advanced (beyond IMT 2000) as the standard for 4G [32].

2G and 3G systems have been designed to use TDMA, FDMA and CDMA as channel access schemes. However, 4G uses OFDMA and other new technologies such as Interleaved FDMA, and Multi-carrier CDMA. 4G also aims to make use of IPv6 instead of IPv4. With IPv6, each device will have its own IP and even when the access point is changed this IP will not. IPv4 suite was designed to use only 32 bits and is capable of addressing up to 4,294,967,269 devices, whereas IPv6 uses 128 bits and is able to address 3.4×10^{38} devices.

IEEE 802.16e standard (“Mobile WiMaX”) and 3GPP standard (LTE) are two main candidates for 4G. In this work we mainly focus on the IEEE 802.16e. IEEE 802.16e and LTE both have adopted OFDMA as their multiple access technique in the physical layer [11] [36]. OFDMA is a multiple access technique to allow multiple users to send and receive data in the same frame and makes use of OFDM modulation. OFDM in general makes use of an even number of carrier frequencies [20]. Each of these carriers is referred to as a sub-carrier. OFDM can tolerate Inter Symbol Interference (ISI) in frequency selective wireless channels. OFDM converts wideband channel into number of narrowband sub-channels with bandwidth considerably lower than coherence bandwidth of the channel B_{coh} [20]. This conversion makes each sub-channel experience flat fading which eventually reduces the complexity of the receiver and converts complex equalization in the receiver to a simple complex multiplication per carrier. The other advantage of OFDM systems is that, as OFDM uses Discrete Fourier Transform (DFT) the system can be

implemented using Fast Fourier Transformation (FFT) and because sub-carriers are orthogonal to each other OFDM can achieve high spectral efficiency.

In OFDMA, each user will be allocated a specific place in a two dimensional plane of time and frequency. In this work we studied OFDMA in the context of IEEE 802.16e (“Mobile WiMaX”). “Mobile WiMaX” uses variation of OFDMA called Scalable Orthogonal Frequency Division Multiple Access (SOFDMA). In SOFDMA sub-carrier spacing between sub-carriers will be constant and set at 10.9375 kHz. This would mean that the possible number of sub-carrier (FFT size) would be determined by the bandwidth of the system. For example in 10 MHz bandwidth any WiMaX system will use 1024 point and in 20 MHz it will use 2048 point FFT.

In “Mobile WiMaX” sub-carriers will be divided into subsets called sub-channels. Sub-carriers in each sub-channel will be chosen based on their sub-carrier permutation mode. There are three permutation modes in “Mobile WiMaX” Partial Usage of Sub-channels (PUSC), Full Usage of Sub-channels (FUSC), and Adjacent Sub-carrier Permutation (AMC). As in SOFDMA the number of sub-carriers depends on the bandwidth of the system and sub-carrier spacing is constant the number of sub-channels is also proportional to bandwidth of the system, for example 30 sub-channel for 10 MHz bandwidth and 60 sub-channel for 20 MHz bandwidth.

SOFDMA has been introduced by WiMaX Forum and it ensures the Interoperability of WiMaX devices from different vendors. IEEE 802.16e standard supports both Time Division Duplexing (TDD) and Frequency Division Duplexing (FDD). “Mobile WiMaX” chooses to use TDD for full duplex communication so time domain

will be divided into 5ms chunks called frames. Each frame contains 48 OFDMA symbol and these are shared between downlink (DL) and Uplink (UL) with a typical ratio of 2:3 as depicted by Figure 1.1.

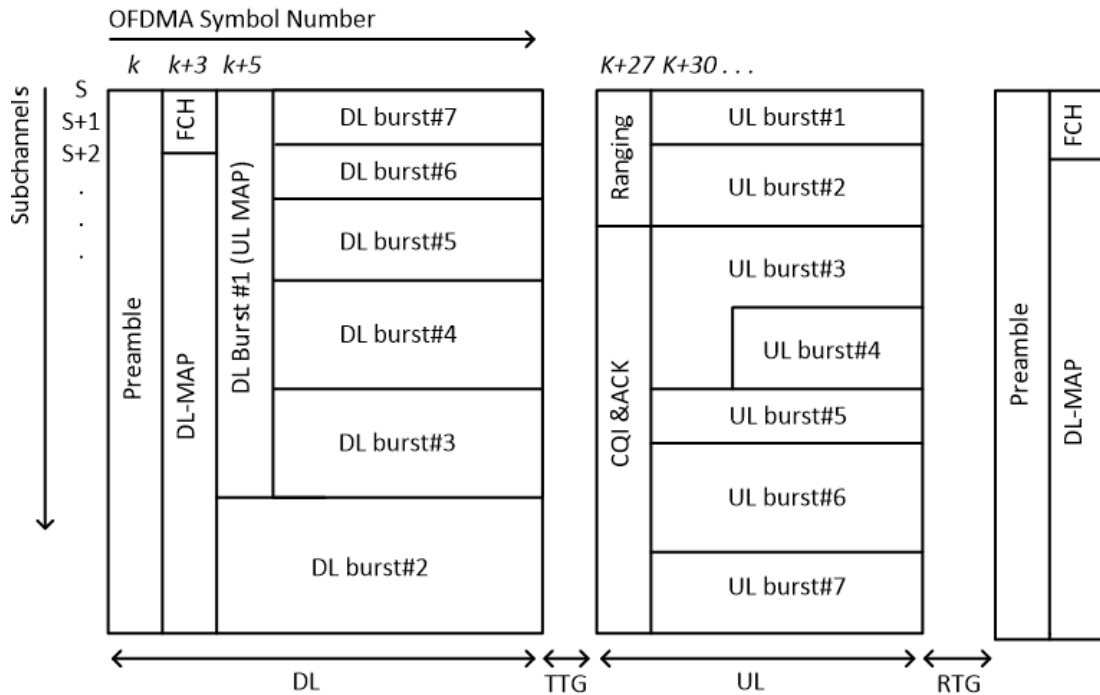


Figure 1.1: WIMAX Frame [1]

The DL for WiMaX dictates that the regions allocated to each user is rectangular. Dimensions of the rectangular regions which are also referred to as bursts are defined by scheduler based on traffic queues and QoS requirements of each individual user [1]. Placement of the rectangular regions into a frame must be done carefully so that unused and over allocated regions are minimized. If placement is done in a haphazard way then the system's throughput will be affected negatively.

While evaluating the performance of frame packing algorithms three main criteria are considered. These include the complexity of the algorithm, the number of unused slots and the number of over allocated slots. As shown in Figure 1.2, based

on traffic queues the scheduler will schedule some arbitrary amount of data per user (in a rectangular fashion) to be packed into the current frame. Based on this, packing algorithms might over allocate some slots to fit the data into the required rectangular shape or in some cases packing algorithm will not be able to fit bursts of particular dimensions into the frame and therefore some slots are left unused. Both the over-allocations and the amount of unused slots have a significant impact on the performance of the packing algorithms and can severely degrade the throughput of a system.

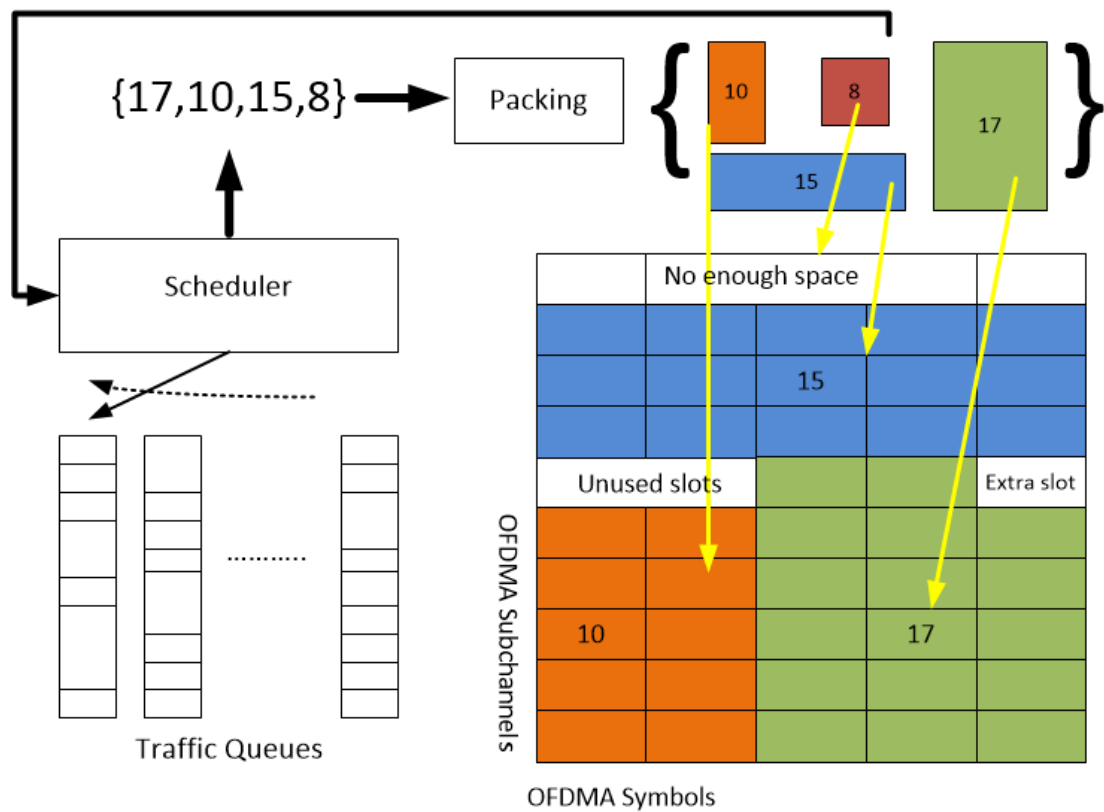


Figure 1.2: Arbitrary data packing example [2]

Until now many packing algorithms have been proposed in the literature. Some of these two dimensional rectangular mapping algorithms are exhaustive search based methods and some others are heuristic algorithms which are practically implementable. Finding a proper heuristic algorithm with a good performance and

acceptable level of complexity is still open to research. eOCSA [3] and Orientation Based Burst Packing (OBBP) algorithm [4] are two heuristic algorithms which have been widely accepted. This work tries to expand on the eOCSA algorithm to propose a new packing algorithm that will provide a lower percentage for the average value for unallocated requests and also tries to combine QoS awareness into the proposed packing mechanism.

1.1 Background

OFDM was first introduced by Chang in 1966 [5]. In a system using OFDM the frequency domain bandwidth is divided into parts called sub-channels. Each sub-channel contains carrier signals called sub-carrier. In [5], parallel transmission was based on banks of oscillators and multipliers in modulator and matched filters in demodulator therefore for a large number of sub-carriers the complexity of the system would be considered high. Weinstein in [6] proposed to use Discrete Fourier Transform (DFT) for modulation and demodulation in OFDM systems. Using DFT reduced the implementation complexity of an OFDM system to an acceptable level for practical purposes. The next milestone for OFDM systems was in early 1980s when Peled [7] introduced using cyclic prefix aided technique in OFDM systems. Through the usage of guard intervals Peled's proposed method would allow OFDM systems to cope nicely with distorted channels and reduce the complexity of the system. In 1980 Keasler described a high-speed OFDM modem for telephone networks [8] and later in 1985 Cimini investigated OFDM for mobile communication [9].

During 1995 European Telecommunications Standards Institute (ETSI) introduced the first Digital Audio Broadcasting (DAB) system using OFDM. Since then many

other standards such as IEEE802.11a, IEEE 802.11g and IEEE 802.16 based on OFDM has been introduced [10]. IEEE 802.16 which was introduced in 2001 considered fixed broadband wireless access between 10 to 66 GHz. Later in 2005 IEEE published the 802.16e standard which is also known as “Mobile WiMaX”. IEEE 802.16e was planned to work in any band between 2 to 66 GHz [11]. Yet another milestone came with the IEEE 802.16m which has been introduced in 2011. IEEE 802.16m standard was the first IEEE standard to fulfill the ITU-R IMT-Advanced requirements on 4G systems.

With the ever increasing demand for OFDMA based 4G technologies, the downlink data packing problem has become an important issue for communication and network engineers. A short literature survey would show that Yehuda Ben-Shimol and his colleagues had proposed for the first time the use of a RASTER algorithm with fragments [12]. This method is known to suffer from DL-MAP overhead and has been shown to be power inefficient as the algorithm allocates bursts row by row and the amount of time (OFDM symbols) that each mobile station will be turned on is not minimized. In [13] Xin Jin had introduced Mapping with Appropriate Truncation and Sort (MATS) algorithm which tried to limit the fragmentation of the RASTER algorithm. In 2008, Wang proposed the Weighted Less Flexibility First (WLFF) algorithm [14]. Where allocation of the bursts was based on the flexibility measure. Later in 2008, Marc C. Necker investigated using a genetic algorithm in the Adaptive Modulation Coding (AMC) mode of IEEE802.16e [15]. In 2009 Chakchai So-In proposed One Column Striping with Non-Increasing Area First Mapping (OCSA) [16] and then through some enhancement and modifications decreased the complexity of OCSA algorithm from $O(n^3)$ to $O(n^2)$ in a new version named

eOCSA [3]. In 2011, Orientation-Based Burst Packing (OBBP) was introduced by Omar M. Eshanta. OBBP is similar to OCSA but it is using matrices to find optimal column or rows to minimize unused slots. The performance of OBBP algorithm depends on the variation between the different bursts and it has been shown that OBBP would perform poorly when the offered load is less than the frame capacity [4] [2] [17].

1.2 Thesis Description

In this thesis we mainly focus on the 2-dimensional frame packing problem for IEEE 802.16e. Our simulations were carried out for PUSC mode which is a mandatory permutation mode for “Mobile WiMaX”. Hata channel model was used in the 2360-2370 MHz band. An urban macrocell environment with a 2000 meter radius was considered as a model where each user’s speed will be uniformly chosen in the range 0 to 60 km/h and Variable Bit Rate (VBR) traffic has been assumed. All simulations were carried out using the MATLAB platform writing dedicated functions whenever necessary. Simulation of the well-known eOCSA packing algorithm has been done assuming 20 users and the above mentioned criteria. Afterward a novel packing algorithm with two extensions to eOCSA was proposed. The first extension simply tries to accommodate bursts that cannot be fitted in their frames in future frames and second extension provides a priority-aware packing mechanism where the leftover bursts are progressively given higher priority numbers in upcoming frames. The two novel algorithms have been simulated and their performance compared with that of eOCSA.

The contents of this thesis have been organized as follows. Following a general introduction, the background survey and the description on how the thesis has been

organized in Chapter 1, Chapter 2 provides description for OFDM and OFDMA and explains how IEEE 802.16e will use these technologies in its physical layer. Chapter 3 introduces the various permutation modes in IEEE 802.16e and then provides details about the PUSC mode. The chapter also provides a graphical user interface for a MATLAB program that can be used to obtain the sub-carrier frequencies in the different sub-channels. Chapter 4 provides details about the COST 231 HATA channel model and shows how path loss and SNR can be computed. A summary of widely known heuristic packing algorithms that include OCSA, eOCSA, OBBP and out novel extensions to eOCSA are given in Chapter 5. The chapter also explains different parameters that we have adopted in our simulations. In Chapter 6 simulation results are provided and discussed. Finally in Chapter 7 conclusions are made and directions for future works are provided.

1.3 Thesis Contributions

The thesis provides a GUI tool to show which indices have been selected for the different sub-channel in the mandatory PUSC mode. Until now no such non-commercial tool has been available. We believe due to the minor ambiguities and typing mistakes in the literature such a GUI will help other new starters to be sure about the integrity of the generated sub-carrier frequency indices. The thesis also proposed two novel packing algorithms which are extensions of eOCSA (Extended eOCSA and Priority-Aware Extended eOCSA). When simulated over the COST 231 HATA channel assuming 20 users the extended eOCSA algorithm would outperform the standard eOCSA. The priority aware extended eOCSA algorithm with two level priority (low: 1-2, high: 3-6) and 20 users would also outperform the eOCSA. Even with 20% increase in the traffic load the Priority Aware Extended eOCSA algorithm can attain an average percentage for unallocated bursts below 3%. A summary of all

the work done in this thesis has been drafted as a paper for SIU2013 conference and the paper has been accepted and published.

Chapter 2

OFDM, OFDMA AND SOFDMA

2.1 FDM

OFDM is considered as the basis for most of today's wideband digital communication systems and handful of wireless standards such as IEEE 802.11 (WIFI), IEEE 802.16e (WIMAX), and LTE-Advanced which has OFDM as its preferred multi-carrier modulation scheme. Multicarrier modulation systems such as the conventional Frequency Division Multiplexing (FDM) would try to divide the available bandwidth W among the N_c sub-carriers with sub-carrier spacing of $\Delta f = W/N_c$. Figure 2.1 illustrates the spectrum for a FDM system.

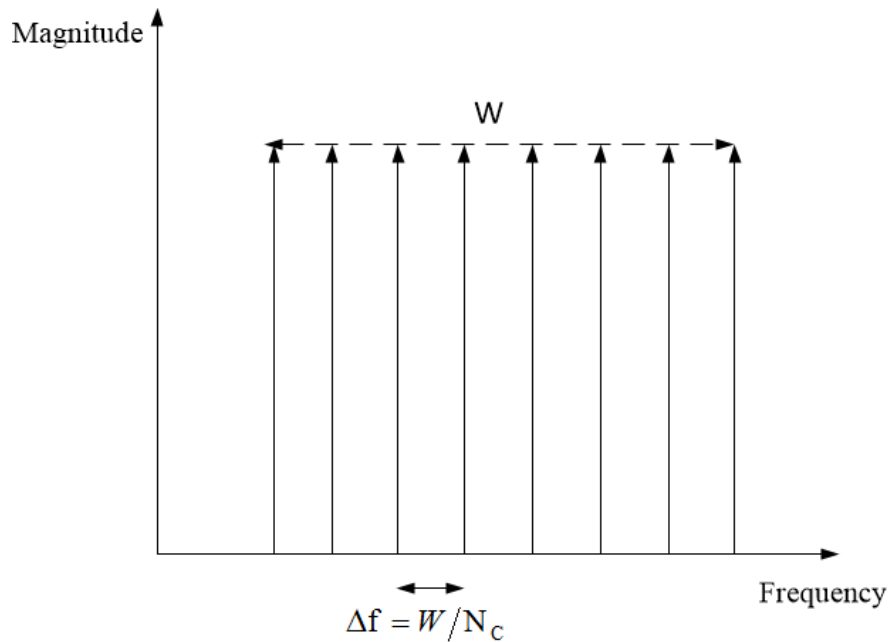


Figure 2.1: Spectrum of FDM [20]

By using multiple carriers FDM would divide a high baud rate (R) data stream into N_c shorter streams and modulate each sub-stream with its own sub-carrier. After the modulation of data sub-streams the symbol duration for each sub-band would be N_c/R and can be made much longer in comparison with the high rate original data stream that has symbol duration $T_s = 1/R$. By choosing N_c appropriately high one can make the symbol duration much longer than the maximum excess delay (τ_{max}) time of the channel and also at the same time would keep the bandwidth of each transmission smaller than coherence bandwidth of the channel (B_{coh}). When the symbol duration is longer than the maximum excess delay the fading could be assumed as quasi-static and equalizers can deal with the Inter Symbol Interference (ISI) much easier. On the other if the coherence time T_{coh} of the channel is smaller than the symbol period of the signal, then the frequency response would change quite fast during the transmission of a symbol and hence reliable detection would be at risk.

By considering all the above it is possible to derive a reasonable range for the number of sub-carriers which one should choose in an FDM system. In fact, [24] had pointed out that N_c is bounded as in (2.1).

$$W/B_{coh} \ll N_c \ll RT_{coh} \quad (2.1)$$

Figure 2.2 and Figure 2.3 are showing the block diagrams for an FDM modulator and demodulator respectively. The main parts of an FDM transmitter are the serial to parallel converter, the oscillators and multipliers and the FDM demodulator makes

use of matched filtering. Unfortunately, for a high number of sub-carriers this would result in a complex and expensive system.

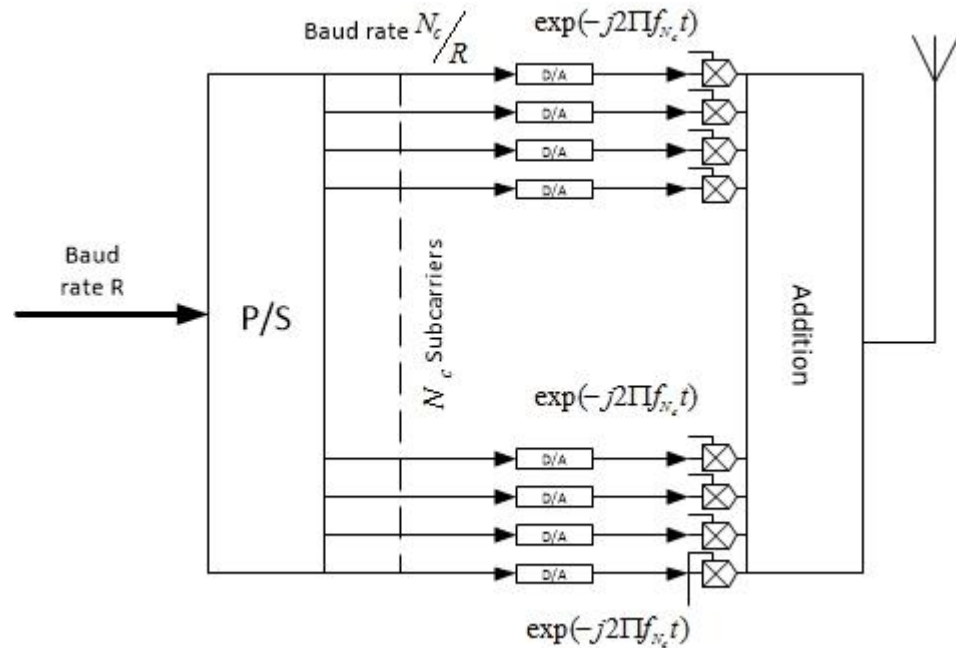


Figure 2.2: FDM Modulation [18]

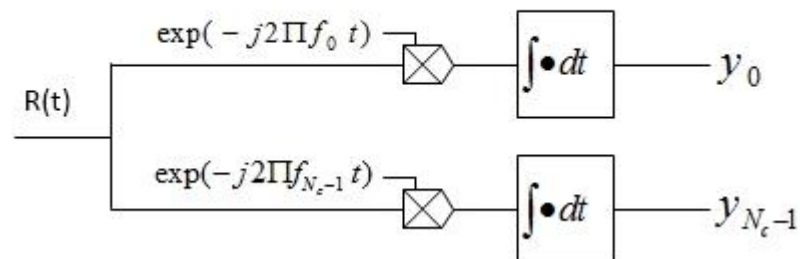


Figure 2.3: FDM Demodulation [20]

2.2 OFDM

FDM systems were using oscillators and matched filters in their design and this issue makes them so expensive and complex to build for large number of sub-carriers. OFDM systems on the other hand are using a mathematical transformation called Discrete Fourier Transform (DFT) in order to modulate and demodulate the data stream [18]. Using this transform has two main advantages; firstly as sub-carriers generated with this method are orthogonal to each other they will not interfere in

frequency domain. Figure 2.4 shows the frequency spectrum of 5 orthogonal sub-carriers. As these sub-carriers are orthogonal there is no need for guard bands between sub-carriers also this orthogonally results in more spectral efficiency than conventional FDM. The second advantage of DFT is that it can be efficiently implemented using Digital Signal Processing (DSP) techniques such as Fast Fourier Transform (FFT).

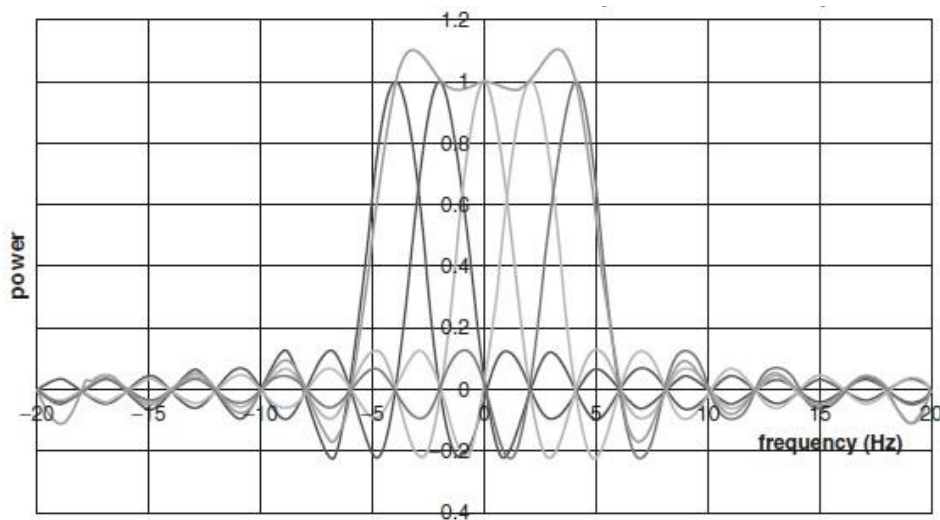


Figure 2.4: Five Sub-carrier OFDM System [19]

A complete block diagram for an OFDM system is shown in Figure 2.5. At first the OFDM system applies IDFT to sub-streams. Afterward the cyclic prefix is added and multiplexed with the outputs of the IDFT block. The OFDM symbol $s(n)$ is then transmitted into the communication channel. At the receiver side the received noisy copy is de-multiplexed and the previously added cyclic prefix is removed. Afterwards, the remaining streams are fed to the DFT block to invert the IDFT effect.

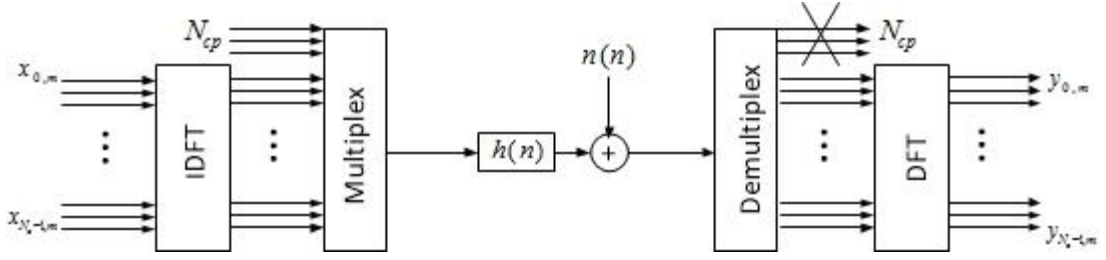


Figure 2.5: OFDM System Diagram [20]

2.2.1 DFT and IDFT and FFT

DFT is a transformation which converts the equally spaced samples of any signal in the time domain into a finite set of complex coefficients of sinusoids with ordered frequencies that are integer multiples of a fundamental frequency. DFT and IDFT can be mathematically denoted as in 2.2 and 2.3, where N is the number of samples.

$$X_k = \sum_{n=0}^{N-1} x_n e^{-i2\pi kn/N} \quad (2.2)$$

$$x_n = \frac{1}{N} \sum_{k=0}^{N-1} X_k e^{i2\pi kn/N} \quad (2.3)$$

The Fast Fourier Transform (FFT) is an effective algorithm for the fast implementation of the DFT. Forward FFT takes a random signal, multiplies it successively by complex exponentials over the range of frequencies, sums each product and plots the results as a coefficient of that frequency. The coefficients are called a spectrum and they indicate how much of that frequency is present in the input signal.

2.2.2 Cyclic Prefix

When a signal passes through a time dispersive channel the timing of the modulated symbols will be distorted and they will start to overlap and interfere with the subsequent symbols. This phenomenon is usually referred to as Inter Symbol Interference (ISI). ISI can reduce the effectiveness of the decision making mechanism at the receiver which will lead to an increase in the Bit Error Rate (BER) and a parallel decrease in the throughput of the system. The effect of ISI in time domain can be seen in Figure 2.6.

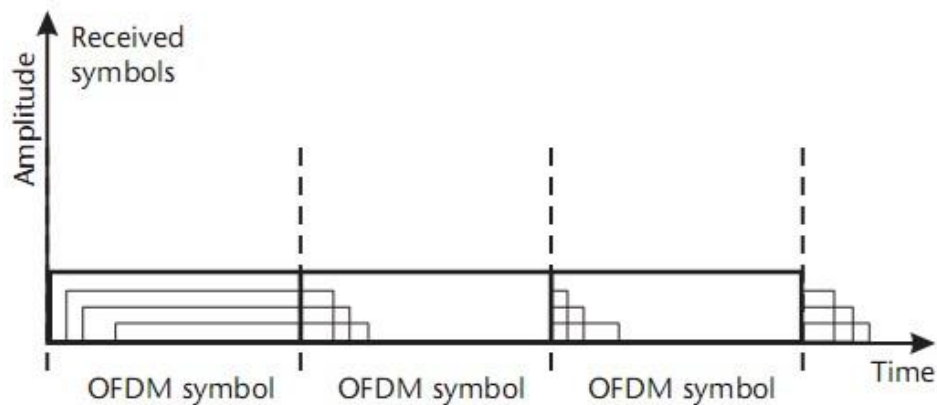


Figure 2.6: Effect of ISI on Symbols [18]

In wireless channels, signal fading is mainly caused by multi-path propagation. The presence of multi-path is either due to atmospheric reflections/refractions or reflections/scattering from buildings, trees and geographical structures. Multi-path implies that many copies of the transmitted signal will reach the receiver and each copy will have a different amplitude and delay. It is possible for the received copies of the signals to add constructively or destructively. When they add destructively this will cause deep fades in the frequency response of the channel and cause severe

attenuation of the transmitted signal. Figure 2.7 shows the frequency response of the fading channel under 100Hz.

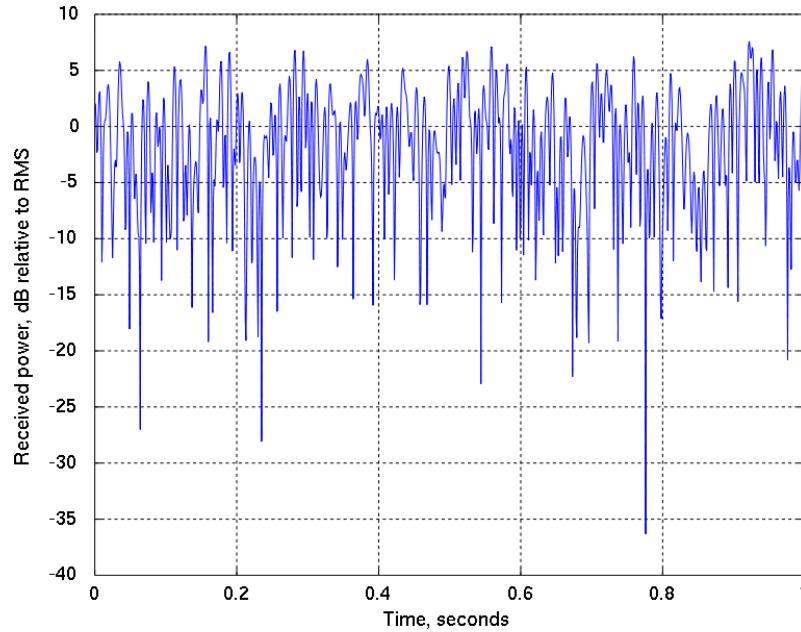


Figure 2.7: Deep Fades in The Frequency Response

In [7] Peled had proposed to use a cyclic prefix in OFDM systems to overcome the effect of ISI. Cyclic prefix is a copy of the last part of the symbol which has been added to the beginning of the symbol. This part works as a guard period for the symbol to eliminate the effect of interference from previous symbol. Cyclic prefix will be added to the transmitted signal after modulation (IFFT block) and will be discarded in the receiver before demodulation (FFT). For cyclic prefix to be effective the length of it should be longer than experienced impulse responds of the channel($\Delta\tau$) [20]. The Signal to Noise Ratio (SNR) loss due to the insertion of the cyclic prefix is given by (2.4):

$$SNR_{loss} = -10 \log_{10} \left[1 - \frac{T_G}{T_s - T_d} \right] \quad (2.4)$$

Figure 2.8 shows how the cyclic prefix is added to an OFDM symbol. The ratio of length of cyclic prefix T_G to useful length of symbol T_d is usually indicated by G. Different values for G can be considered based on the channel conditions. Specific values for G defined by “Mobile WiMaX” physical layer are G: 1/4, 1/8, 1/16 and 1/32 and G= 1/4 is mandatory in OFDMA profile [21].

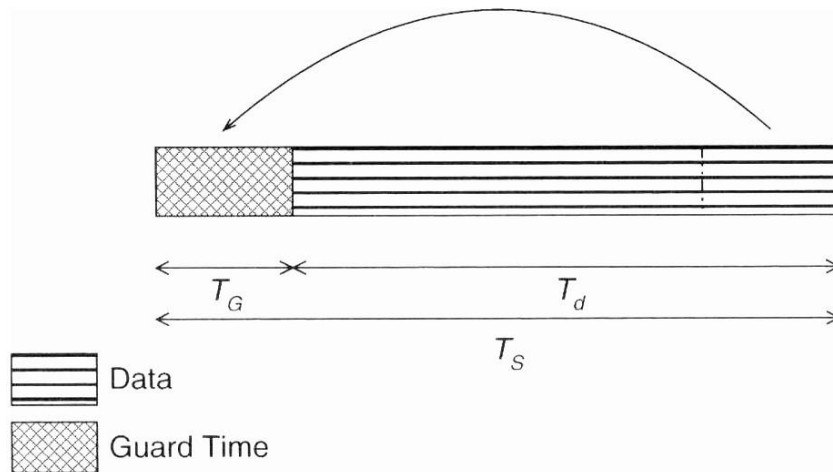


Figure 2.8: Cyclic Prefix in Time Domain [21]

2.3 OFDMA And SOFDMA

OFDMA is a multiple access scheme based on OFDM. In OFDMA the OFDM signal will be generated from signals of many users. OFDMA divides frequency domain into parts called sub-channel. Each sub-channel is a set of sub-carriers, in downlink each sub-channel might be allocated to a user or group of users and in uplink one or more sub-channel may be intended for one transmitter. So each user will have a time and sub-channel allocated (burst) for each one of their requests, An Example of OFDMA has been shown in Figure 2.9.

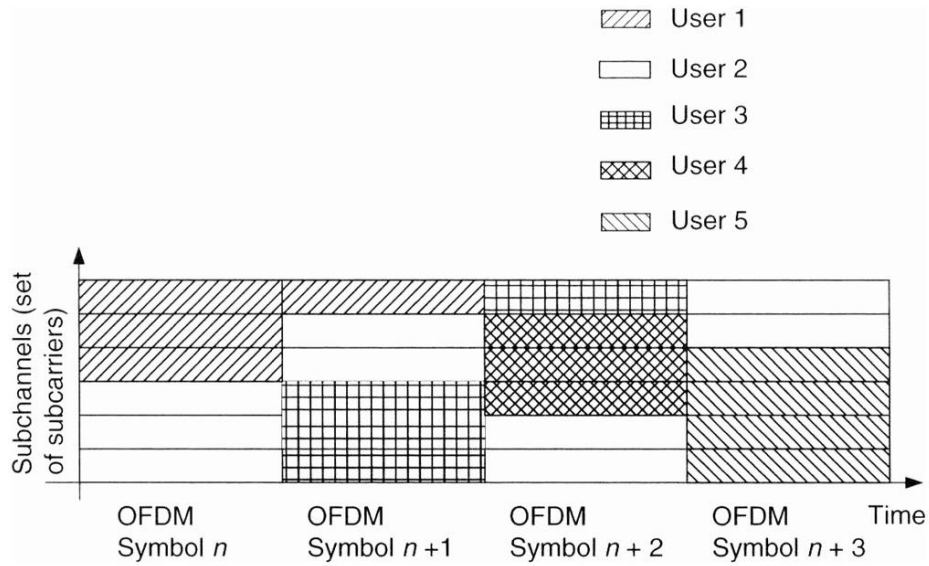


Figure 2.9: Example of OFDMA [21]

Scalable Orthogonal Frequency Multiple Access (SOFDMA) is a variation of OFDMA which has been used in IEEE 802.16e physical layer. In SOFDMA the sub-carrier spacing and useful symbol duration are constant and has been set accordingly to 10.95 kHz and 91.4 μ s. As indicated before in section 2.2.2 $G = 1/4$ is mandatory in “Mobile WiMaX”. In SOFDMA time will be divided into 5ms parts called frames while each frame contains 48 OFDMA symbol with length 102.9 μ s. Using SOFDMA in “Mobile WiMaX” other than providing scalability also ensures the interoperability of WiMaX devices from different vendors. Table 2.1 shows the main parameter for SOFDMA in “Mobile WiMaX” [21].

Table 2.1: SOFDMA Parameter For “Mobile WiMaX” [21]

Parameters	Numerical values	
Sub-carrier frequency spacing	10.95 kHz	
Useful symbol duration ($T_d = 1/\Delta f$)	91.4 μ s	
Guard time ($T_G = T_d/8$)	11.4 μ s	
OFDMA symbol duration ($T_s = T_d + T_G$)	102.9 μ s	
Number of OFDMA symbols in the 5 ms frame	48	
FFT size (N_{fft}) or number of sub-carriers	512	1024
Channel occupied bandwidth	5MHz	10MHz

2.3.1 Sub-channelization

In SOFDMA the sub-carrier spacing is constant and the number of sub-carrier (FFT points) is also proportional to the occupied bandwidth. The supported FFT sizes are 2048, 1024, 512 and 128. FFT size 256 (of the OFDM layer) is not included in the OFDMA layer. Only 1024 and 512 are mandatory for “Mobile WiMaX” profiles. As depicted in Table 2.1 for the 5 MHz channel there are 512 sub-carriers and for the 10 MHz channel there are 1024 sub-carriers. In IEEE 802.16e each Mobile Subscriber (MS) is allocated only a subset of the sub-carriers. The available sub-carriers are grouped into sub-channels (a set of sub-carriers determined by a permutation) and the MS is allocated one or more sub-channels for a specified number of symbols. The process which maps the logical sub-channel to multiple physical sub-carriers is called a permutation. For IEEE 802.16e there are two types of permutation modes; namely the distributed permutation mode and adjacent permutation mode. While the distributed permutation mode is suitable for mobile users the adjacent permutation mode is generally used for fixed (stationary) users.

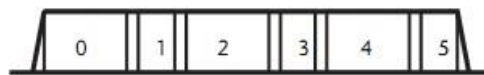
In distributed permutation mode sub-carriers of the sub-channel will be chosen pseudo randomly distributed across the frequency spectrum. Distributed permutation

mode makes use of frequency diversity by distributing the sub-carriers across frequency spectrum. Using distributed permutation modes can help users achieve better performance in a frequency selective fading channel or broadcasting the control information (downlink map) to all users in the frame where frequency selective scheduling is not applicable. By using distributed permutation modes the probability of using the same sub-carrier in adjacent sectors or cell will be minimized but as sub-carriers are distributed across spectrum good channel estimation would be much harder to achieve [21].

In the adjacent permutation mode sub-carriers of sub-channels are subsequent to each other in the frequency spectrum. This makes the channel estimation easier compared to distributed permutation mode. While adjacent permutation mode would not benefit from frequency diversity, it uses another form of diversity called multi-user diversity. In adjacent permutation mode each user will be allocated sub-channels that maximize the Signal to Interference and Noise Ratio (SINR) of that given user. Using multi-user diversity can provide significant gain in the throughput of the system [22]. Adaptive Modulation and Coding (AMC) is the adjacent permutation mode in “Mobile WiMaX”. This mode is suitable for using Adaptive Antenna System (AAS) in “Mobile WiMaX”.

Partially Usage of Sub-channels (PUSC) and Full usage of Sub-channels (FUSC) are two main distributed permutation modes in “Mobile WiMaX” [22]. In FUSC permutation mode sub-carriers of any given sub-channel can be chosen from all available sub-carriers across spectrum. This method achieves full frequency diversity. On the other hand, in PUSC permutation mode sub-carriers firstly has been

divided into groups (segments) and then mapped to sub-channels based on their segments. This segmentation allows the service providers without sufficient spectrum to be able to afford frequency reuse factor $N=1$ without severe adjacent cell interference [18]. Figure 2.10 shows possible allocation of groups to sectors of base station in order to achieve frequency reuse factor $N=1$.



(a)

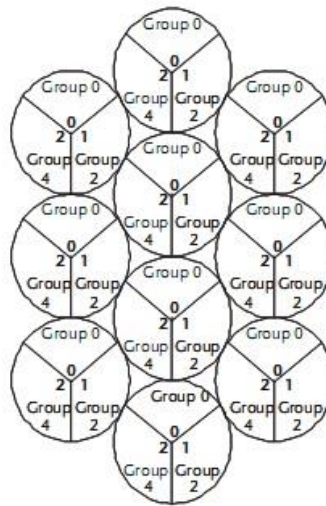


Figure 2.10: Example of Using Segmentation with Frequency Reuse Factor $N=1$ [18]

Chapter 3

DL-PUSC: A DISTRIBUTED PERMUTATION MODE FOR WIMAX

3.1 Downlink PUSC

PUSC is the mandatory permutation mode used by “Mobile WiMaX” standard. PUSC permutation mode makes use of frequency diversity and tries to minimize the adjacent cell interference by virtually sectoring the cell into segments. This chapter will provide an in depth explanation for the calculations required by the PUSC permutation mode and will also introduces a MATLAB based GUI to find sub-carrier physical indices of each sub-channel easily.

PUSC is a distributed permutation mode for IEEE 802.16e and slot is the smallest possible data allocation unit for “Mobile WiMaX”. In downlink PUSC (PUSC-DL) each slot consists of one sub-channel over two consecutive OFDM symbols where each sub-channel consists of 24 sub-carriers. A burst is a rectangular data allocation region over multiple sub-channels and OFDM symbols. Another term which has been used in PUSC methodology is segment. Segment is a set of available sub-channels. Each cell in PUSC-DL consists of three segments. Each of these segments belongs to one sector of the base station. In PUSC-DL, DC sub-carrier has a frequency that is equal to RF center frequency of the base station.

Another important term for distributed permutation mode is the “Permutation Base”. This parameter is separately defined for DL and UL communication. In DL it is known as DL-PermBase. The possible values for DL-PermBase range from 0 to 31. The value of the DL-PermBase identifies the particular segment used (by the base station). DL-Perm Base is specified by MAC layer [23]. For IEEE 802.16e which makes use of SOFDMA a 10 MHz channel corresponds to 1024 sub-carriers (FFT points). These 1024 sub-carriers are numbered accordingly from 0 to 1023. These numbers in the literature of WiMaX are known as absolute sub-carrier indices.

In a 1024 points FFT system there are 183 guard sub-carrier, (92 on the left side and 91 on the right hand side) and 1 DC sub-carrier. After subtracting all of these guards and DC sub-carrier there will be 840 sub-carriers remaining. These sub-carriers are for data plus the pilots used for synchronization (used sub-carriers). These used sub-carriers are grouped into sets of 14 adjacent sub-carriers called physical clusters. There are 60 physical clusters in a 1024 point OFDM system. Figure 3.1 shows sub-carriers and clusters for a 1024 point FFT system. In SOFDMA there are three types of sub-carriers: data sub-carriers for data transmission, pilot sub-carriers for channel estimation and null sub-carriers. Guard band sub-carriers and DC sub-carriers are considered as null sub-carriers.

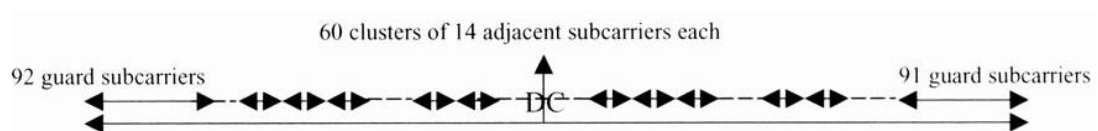


Figure 3.1: Sub-carriers in The 1024 FFT [21]

The permutation process of PUSC-DL to form sub-channels can be described in five main steps. In first step sub-carriers will be partitioned and the used sub-carriers will be identified. Afterward these used sub-carrier (840 sub-carriers in 1024 FFT case) will be divided into groups of 14 adjacent sub-carriers to form physical clusters. A “Mobile WiMaX” system with 1024 point FFT would have 60 clusters (numbered 0-59). These physical clusters include all the data and pilot sub-carriers. In second step, physical clusters from first step will be re-numbered using (3.1) and the re-numbering sequence provided in (3.2) to form logical clusters. This step is known as outer permutation. The length of the renumbering sequence is always equal to the number of clusters. The re-numbering sequence for a 1024 point FFT with 60 clusters is as stated in [21] and has been given in (3.2).

$$\text{Logical Cluster} = \{[\text{Renumbering Sequence (Physical Cluster)} + 13 \cdot \text{DL-Perm Base}] \% (\text{number of clusters})\} \quad (3.1)$$

$$\begin{aligned} \text{Renumbering sequence} = & [6, 48, 37, 21, 31, 40, 42, 56, 32, 47, 30, 33, \\ & 54, 18, 10, 15, 50, 51, 58, 46, 23, 45, 16, 57, 39, 35, 7, 55, 25, 59, 53, \\ & 11, 22, 38, 28, 19, 17, 3, 27, 12, 29, 26, 5, 41, 49, 44, 9, 8, 1, 13, 36, 14, \\ & 43, 2, 20, 24, 52, 4, 34, 0] \end{aligned} \quad (3.2)$$

Figure 3.2 shows the absolute sub-carrier indices for each one of the 1024 sub-carriers when the “DL-PermBase” is set to zero. The effect of the outer permutation can be easily identified among 840 used sub-carriers.

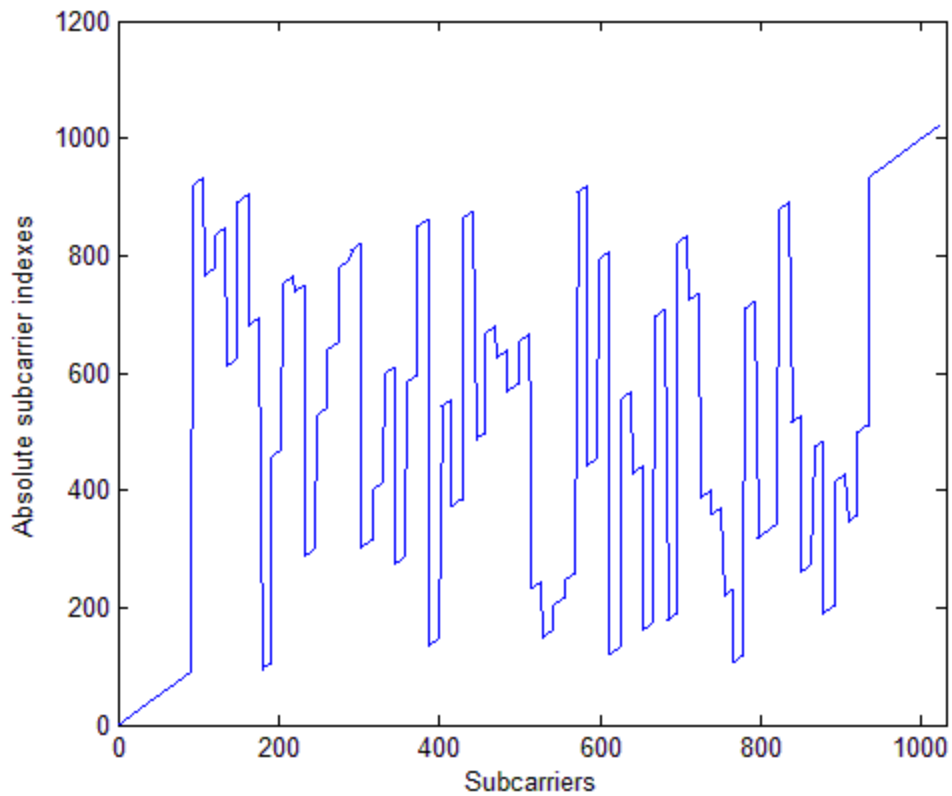


Figure 3.2: Absolute Sub-carrier Indices of Sub-carriers in 'PermBase 0'

In the third step, logical clusters are grouped together to make six major groups. These major groups are numbered starting from 0 to 5. For a 1024 point FFT each even major group contains *twelve* logical cluster and each odd major groups contains *eight* clusters. In PUSC-DL one sub-channel does not have sub-carriers from more than one major group [21]. The major groups and their correspondent sub-channels are shown in Table 3.1. In the fourth step, positions of the pilot sub-carriers will be marked individually for odd and even OFDM symbols. Pilot sub-carriers for odd OFDM symbols will be the 4th and 8th sub-carriers for each logical cluster (numbered 0 to 13). For the even OFDM symbols pilots will be the 0th and the 12th in a logical cluster. Figure 3.3 shows the location of pilots in logical cluster number zero.

Table 3.1: Major Groups and Their Sub-channels

Major Group	Sub-channel Range
0	0-5
1	6-9
2	10-15
3	16-19
4	20-25
5	26-29

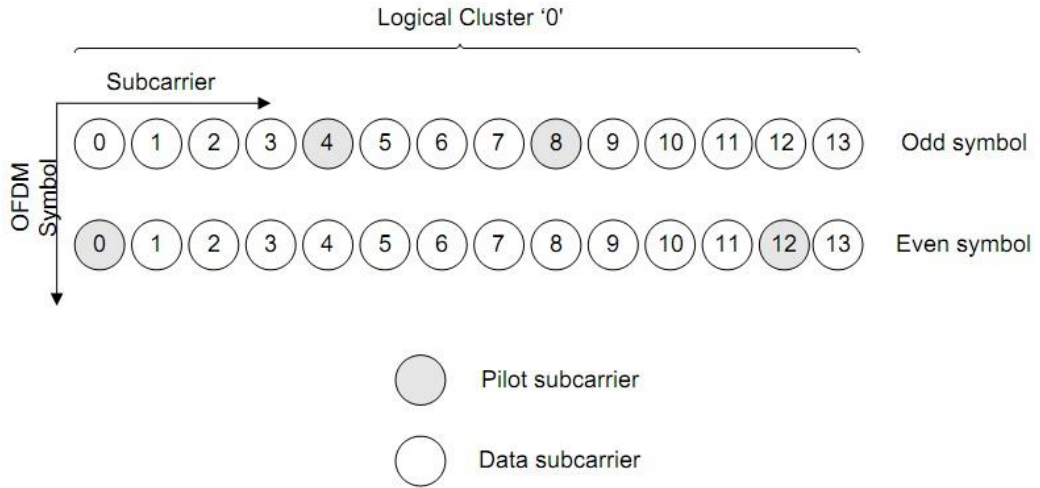


Figure 3.3: Pilot Sub-carriers of Logical Cluster 0 [23]

In the last step sub-carriers of each group are assigned to sub-channels. Sub-carriers will be assigned using (3.3) and (3.4).

$$Subcarrier(k, s) = N_{subchannels} * n_k + \quad (3.3)$$

$$\{P_s[n_k \bmod N_{subchannels}] + DL - PermBase\} \bmod N_{subchannels}$$

$$n_k = (k + 13s) \bmod N_{subcarriers} \quad (3.4)$$

This process is known as the inner permutation. The indices obtained using (3.2) are the group sub-carrier indices of the sub-carriers. Group sub-carrier index is an index

for data sub-carriers of each individual group ranging from 0 to 143 for even numbered major groups and ranging from 0 to 95 for odd numbered major groups.

In (3.2) and (3.3), $Subcarrier(k,s)$ is group sub-carrier index of sub-carrier k . S is the index number of sub-channel from 0 to 29 for the 1024 FFT PUSC-DL. $N_{subchannels}$ denotes the number of sub-channels in a group and for even and odd groups is 12 and 8 respectively. K is sub-carrier in sub-channel index ranging from 0 to 23 in PUSC-DL. In (3.3) $N_{subcarriers}$ is number of sub-carrier in the sub-channel which in PUSC-DL is always equal to 24. $P_s[.]$ is a series obtained by cyclically rotating the basic permutation sequence s times to the left. The permutation sequences for even and odd numbered groups are $PermutationBase6 = [3,2,0,4,5,1]$ and $PermutationBase4 = [3,0,2,1]$. Figure 3.4 shows the absolute sub-carrier indices for sub-carriers of sub-channel zero for an even OFDM symbol when DL-PermBase is assumed to be zero. The effect of combination of inner permutation and outer permutation can be seen in this figure. The exact absolute sub-carrier index value for each sub-carrier has been provided in Table 3.2 for this specific case.

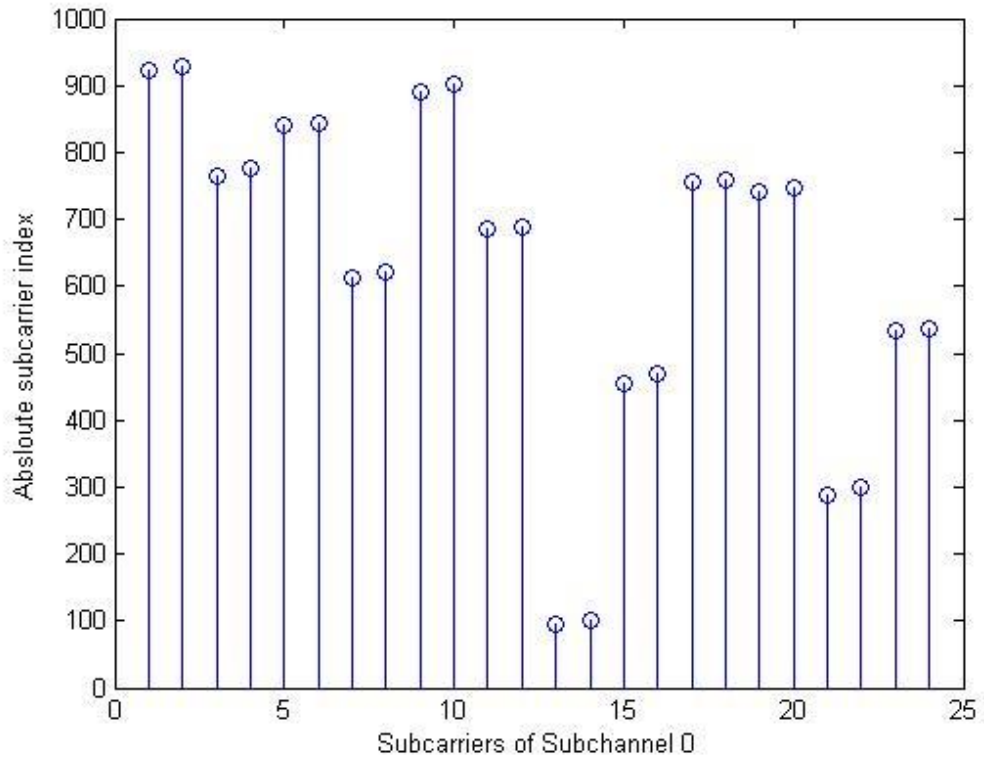


Figure 3.4: Absolute Sub-carrier Indices for Sub-carriers of 'Sub-channel 0'

Table 3.2: Absolute Sub-carrier Indices of 'Sub-channel 0'

Sub-carrier's Index in Sub-channel	Absolute Sub-carrier Index	Sub-carrier's Index in Sub-channel	Absolute Sub-carrier Index	Sub-carrier's Index in Sub-channel	Absolute Sub-carrier Index	Sub-carrier's Index in Sub-channel	Absolute Sub-carrier Index
1	922	7	614	13	95	19	740
2	929	8	621	14	102	20	747
3	765	9	891	15	456	21	288
4	777	10	903	16	468	22	300
5	841	11	687	17	757	23	533
6	844	12	690	18	760	24	536

3.2 MATLAB GUI

To facilitate automated calculation of the exact absolute sub-carrier index value for each sub-carrier in each sub-channel we have written the necessary MATLAB functions and have created a Graphical User Interface (GUI) so anyone could easily produce the index values. Some screen shots from the created GUI based program can be seen in Figure 3.5 and 3.6. This GUI calculates the major group and absolute subcarrier indices of required subcarrier and 'all of the subcarriers' in the same sub-channel based on specified inputs.

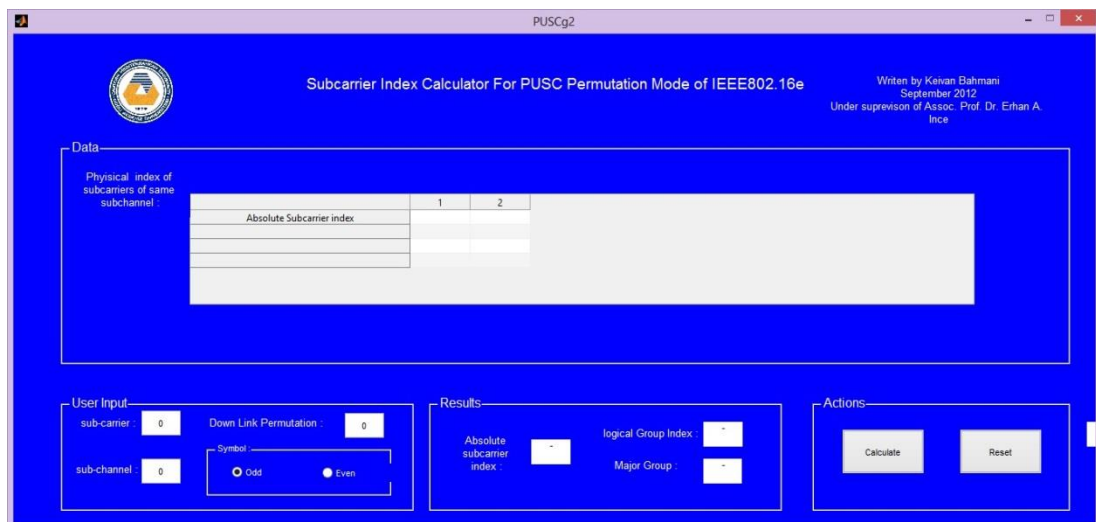


Figure 3.5: GUI for PUSC-DL Calculations

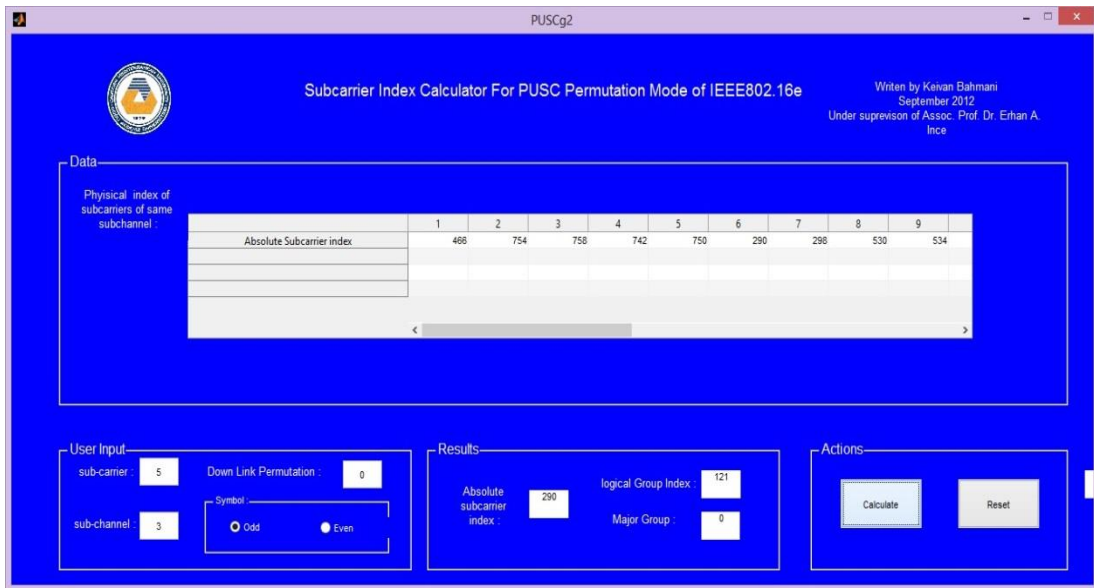


Figure 3.6: GUI Showing The Absolute Subcarrier Indices for Subcarrier 5 of Sub-channel 3 for an ODD OFDM Symbol

Chapter 4

COST-231 HATA Channel MODEL FOR IEEE 802.16E

4.1 COST-231 Hata Model Path Loss

In this work we adopted the COST-231 HATA model as our channel model. COST-231 HATA model is an extension to Hata-Okumura model which has been proposed by Hata in 1981. The original HATA model supported range of frequencies from 150 MHz to 1500 MHz and up to 20 Km distance between transmitter and receiver antenna. The height of transmitter and receiver antenna can vary between 30 to 200 meter for transmitter and 1 to 10 meter for receiver [24].

COST-231 HATA model was proposed to extend the frequency range of Hata model up to 2000 MHz. This model considers three different environments (urban, suburban, and rural) for calculating the path loss [25]. The path loss calculations consist of three main parts. As shown in (4.1) these are respectively the initial offset parameter E_0 the initial system design parameter E_{sys} and the slope of the model curve, β_{sys} .

$$PL(\text{dB}) = E_0 + E_{sys} + \beta_{sys} \quad (4.1)$$

The total path loss can be calculated by substituting (4.2), (4.3) and (4.4), into (4.1).

$$E_0 = 46.3 - ah_m + c_m \quad (4.2)$$

$$E_{sys} = 33.9 \log_{10}(f) - 13.82 \log_{10}(h_b) \quad (4.3)$$

$$\beta_{sys} = (44.9 - 6.55 \log_{10}(h_b)) \log_{10}(d) \quad (4.4)$$

h_b and h_r are the heights of the base station and mobile station antennas above ground in meters. f is the working frequency of the system in MHz and d is the distance between base station and mobile station in kilometers. Parameters ah_m and c_m are known as correction parameters. These correction parameters are based on the environment assumed (urban, suburban) and their values can be found in (4.5) for urban environment and (4.6) for suburban environment. The value for parameter c_m is fixed at 3dB for urban environments and 0dB for suburban environments.

$$ah_m = 3.2(\log_{10}(11.75h_r))^2 - 4.97 \quad (4.5)$$

$$ah_m = 1.1 \log_{10}(f - 0.7)h_r - (1.56 \log_{10}(f - 0.8)) \quad (4.6)$$

In our simulations we have chosen to use the COST-231 HATA model for a macrocell of radius 2000 meter in an urban region. Figure 4.1 shows the path loss calculated vs. distance in a range of 100 - 2000 meters. The antenna heights from the ground were assumed to be 20 meter for base station and 2 meter for mobile station(s).

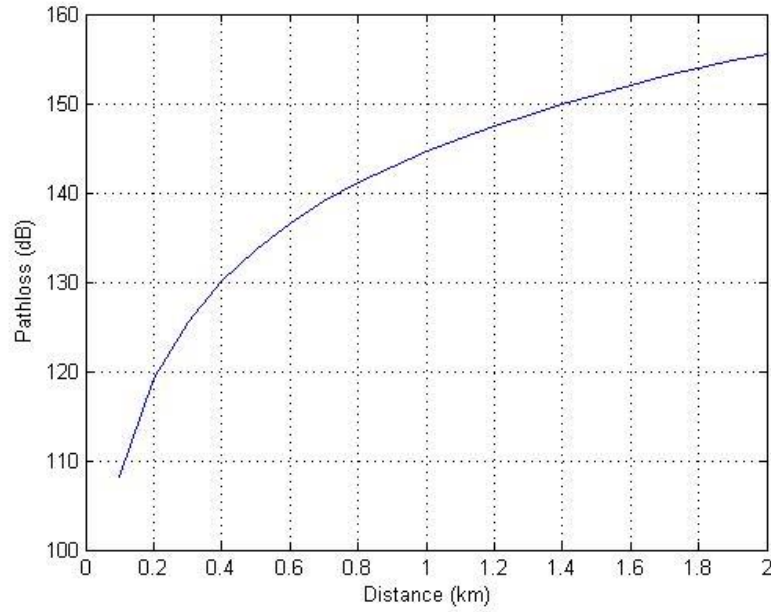


Figure 4.1: Path Loss Calculated With COS-231 Hata Model

4.2 Macro Cell Urban Environment

In this work the environment has been assumed to be one base station in a macro cell urban area. The radius of our macro cell is 2000 meter. The initial distance between each mobile station and the base station has been chosen uniformly distributed in the range of 100 to 2000 meter from the base station. Each mobile station was assumed to move towards or away from the base station with a speed of 0-60 Km/h chosen from a uniform distribution. The location of each user will be estimated for each frame period (5ms) and the path loss will be calculated using COST-231 Hata model.

Table 4.1: Parameter Used in Simulation

Parameter	Setting
Transmitter Antenna Height	20 meter
Receiver Antenna Height	2 meter
Base Station Transmitter Power	16dBW
Base Station Antenna Gain	15dBi
Mobile Station Antenna Gain	0dBi
Total Noise Power at Receiver	-126dBW

Using the path loss calculated with COST-231 Hata model in the previous section and parameters from Table 4.1 the Signal to Noise Ratio of each mobile station can be calculated using (4.7) [34] where P_T denotes the transmission power of the base station G_T is the gain of the base station antenna G_R is the gain of the mobile station antenna and N denotes the total noise power at the receiver.

$$SNR = \frac{P_T G_T G_R}{PL \cdot N} \quad [34] \quad (4.7)$$

SNR calculated based on (4.7) for different distances can be seen in Figure 4.2.

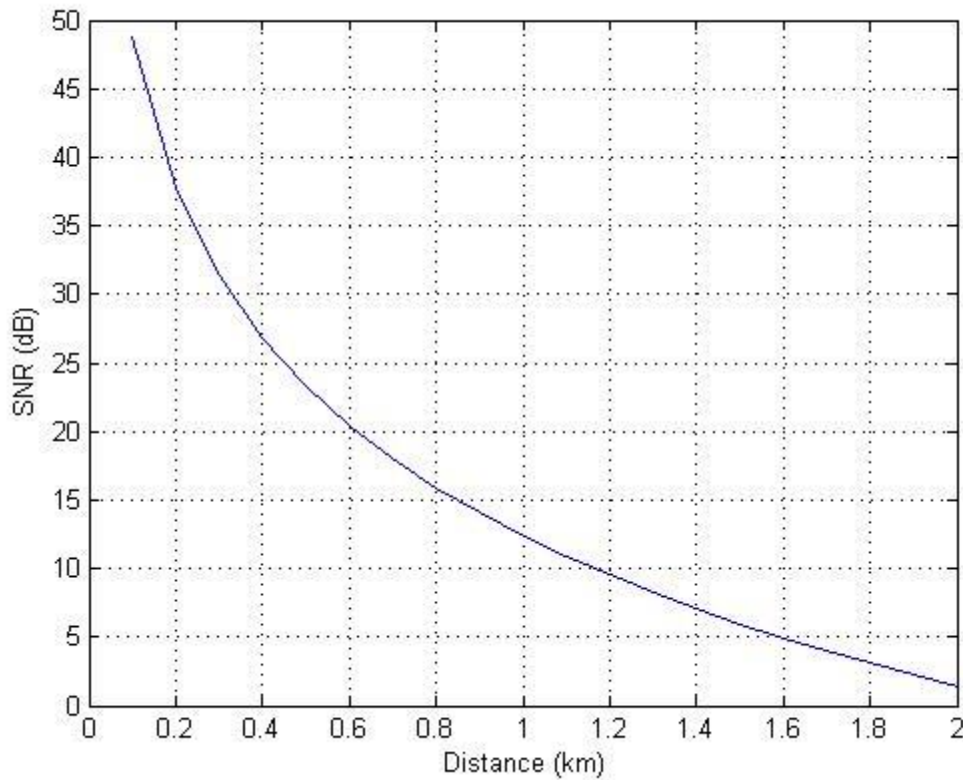


Figure 4.2: SNR for Different Distances

4.3 Modulation and Coding Scheme (MCS) In IEEE 802.16e

“Mobile WiMaX” makes use of adaptive Modulation and Coding Scheme (MSC) to maximize the throughput. The Idea behind adaptive modulation is very simple. WiMAX system will try to transmit with higher modulation level when the channel is good, and transmit with lower and more robust modulations when the channel is poor. In “Mobile WiMaX” Quadrature Phase Shift Keying (QPSK), 16 points Quadrature Amplitude Modulation (16QAM) and 64 points Quadrature Amplitude Modulation (64QAM) are mandatory modulations for the base station. For the mobile stations only QPSK, 16QAM are mandatory modulations [26]. “Mobile WiMaX” also uses Forward Error Correction (FEC) in order to make communications as reliable as possible. Convolutional codes with rates $1/2$, $2/3$ and $3/4$ are supported [21].

“Mobile WiMaX” benefits from burst profiles. These burst profiles are pre-defined sets of modulation levels and coding rates. Using these burst profiles allows the system to find an appropriate threshold between spectral efficiency and reliability for each user and allows the base station to change each user’s profile in the frame. In each frame 2 indices called downlink interval usage code (DIUC) and uplink interval usage code (UIUC) specify which burst has been used in downlink and uplink for each user [18]. Table 4.2 shows burst profiles suggested by IEEE 802.16-2004 standard for BER of 10^{-6} in an Additive White Gaussian Noise (AWGN) channel.

In “Mobile WiMaX” base station use the SNR value of users and choose appropriate burst profile for each user in downlink. Based on these burst profiles the BS knows

the amount of data that can be transferred in each slot of the downlink part of frame (DL bytes/slot). These amounts can be calculated using the formula in (4.8).

Table 4.2: Burst Profiles from IEEE 802.16-2004

Modulation	Coding rate	Receiver SNR threshold (dB)
BPSK	1/2	6.4
QPSK	1/2	9.4
QPSK	3/4	11.2
QAM-16	1/2	16.4
QAM-16	3/4	18.2
QAM-64	1/2	22.7
QAM-64	3/4	24.4

$$\text{DL byte/slot} = \frac{48 \times \text{Bits/symbol} \times \text{Coding Rate}}{8} \quad (4.8)$$

After the BS calculates the required number of slots for each user in the frame the scheduler will tell a packing algorithm the burst dimensions for the allocation of each user and the packing algorithm will try to optimize the fitting of these bursts into the current frame. Table 4.3 shows some of the burst profiles and their correspondent bytes per slot value in PUSC mode of ‘‘Mobile WiMaX’’.

Table 4.3: DL Byte/Slot for ‘‘Mobile WiMaX’’ in PUSC Mode.

Modulation Type	Coding Rate	SNR(dB)	DL bytes/slot
QPSK	1/2	5	6
QPSK	3/4	8	9
16QAM	1/2	10.5	12
16QAM	3/4	14	18
64QAM	1/2	16	18
64QAM	2/3	18	24
64QAM	3/4	20	27

Chapter 5

FRAME PACKING ALGORITHMS

As we have indicated in chapter 2 “Mobile WiMAX” makes use of SOFDMA where each user is allocated a number of sub-channels vs. symbols in frequency and time. For the downlink part of the frame the base station will calculate the number of slots (area of the burst) for each user based on the burst profiles (ref to Table 4.2 in chapter 4). IEEE 802.16e dictates that these bursts be rectangular. Once the burst areas are determined then a frame packing algorithm tries to fit the rectangular bursts into the DL part of the frame in such a way that it minimizes the power consumption of mobile stations, minimizes the over allocations (extra slots require to make burst rectangular), and minimizes the unused slots in the frame.

The problem of packing these burst into a frame is known as two-dimensional rectangle mapping problem. This problem can be considered as a variation of bin packing problem. These classes of mathematical problems are known to be NP-complete which means the complexity of the solution grows exponentially with the number of objects [27]. In 2007, Claude Desset reported that only a limited number of users (maximum 8 users) can be supported with an exhaustive binary-tree full search algorithm [28]. To overcome this problem various heuristic algorithm have been proposed. This chapter consists of explanation for some of these heuristic algorithms and introduces our proposed algorithm which extends the well-known eOCSA algorithm and also introduces the priority concept to deal with QoS.

5.1 OCSA

OCSA has been introduced in 2009 by Chakchai So-In in [16]. OCSA algorithm divides the packing problem into two parts. In the first part a scheduler calculates the slot requirement of each user in the frame based only on their demand and quality of service requirements and available resources. This first part is independent of the rectangular packing mechanism. Afterward OCSA algorithm will allocate burst in three steps as follows; given a set of resources $\{A_i\}$ in the first step OCSA algorithm sorts the set in descending order and starts allocating from the highest value. This helps to maximize the throughput. In the second step OCSA choses the highest elements which can be fitted in the unused space of downlink part of the frame. In this step OCSA calculates all the possible width and height pairs such that $W_{ij} \cdot H_{ij} = A_i$. For example, for the case of $\{A_i\} = 40$ Table 5.1 shows all the width-height pairs. Since some of these pairs are exceeding the size of DL sub-frame, they will be automatically discarded.

Table 5.1: Width and Height Pairs Calculated By OCSA for $\{A_i\} = 40$

Width	1	2	4	5	8	20	40
Height	40	20	10	8	5	2	1

After the algorithm finds all of the feasible pairs for $\{A_i\}$ it chooses the pair with smallest width. This will allow the mobile station to turn off its electronic circuits for the remainder of the DL sub-frame [16].

If there is no feasible mapping pair for certain $\{A_i\}$, the OCSA will choose a pair with least over allocation. For example for $\{A_i\} = 37$ all the determined values with

their respective over allocations can be seen in Table 5.2. In this case the OCSA algorithm chooses the width and height pair that has the least over allocation (in this case 2 and 19).

Table 5.2: Width and Height Pairs Calculated By OCSA for $\{A_i\} = 37$

Width	2	3	4	5	6	7	8	9	10	11	12
Height	19	13	10	8	7	6	5	5	4	4	4
Over allocation	1	2	3	3	5	5	3	8	3	7	11

When the algorithm has determined the appropriate pair for $\{A_i\}$, then the corresponding rectangular burst will be mapped into the frame in a right to left and bottom to top fashion. This step is generally referred to as the horizontal mapping.

After administering the horizontal mapping step, there might be some unallocated slots left above the current allocated burst. To reduce the number of unused slots OCSA will try to allocate extra burst into this remaining space. This step in OCSA is known as vertical mapping. The OCSA algorithm will find the largest allocation that can be fitted into the left-over area in the strip above the most recently allocated burst. Throughout vertical mapping process smaller heights and larger widths (not exceeding the width of the column) will be preferred in an attempt to improve the utilization. Figure 5.1 shows the packing in a frame using the described OCSA algorithm. Computational complexity of OCSA has been stated as $O(n^3)$ where n is the number of resource allocations. It has been shown that OCSA can provide up to 95% throughput compared to a full search algorithm [16].

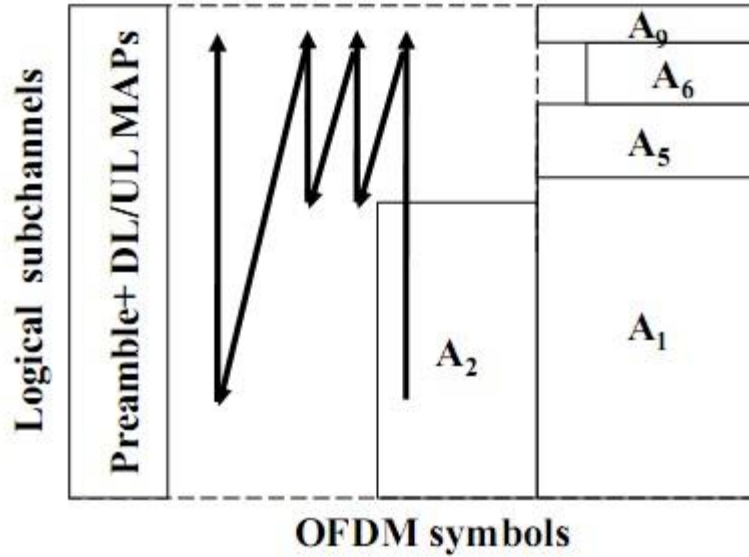


Figure 5.1: Example of Frame Packed Using OCSA [16]

5.2 eOCSA

eOCSA [3] is the enhanced version of the OCSA algorithm. As showed in the previous section OCSA determines all the possible pairs of W_{ij} and H_{ij} for each allocation and then choses the one with the least width. On the other hand eOCSA will consider only the best mapping pairs for each allocation either the least width or the least height. By adopting this method eOCSA reduced the complexity of OCSA from $O(n^3)$ to $O(n^2)$ where n denotes the number of resource allocations within the frame. eOCSA algorithm has three main parts. In the first part it uses a similar sorting technique to that of OCSA and sorts all allocation in descending order to maximize the throughput. Afterwards for the given allocation of area $\{A_i\}$ it uses (5.1) and (5.2) to finds an appropriate width W_i and height H_i for the burst. In (5.1) H corespondes to the maximum available height and in “Mobile WiMAX” with 10 MHz bandwidth H is equal to 30. Based on (5.1) one can see that eOCSA tries to

minimize W_i so that the active time of the mobile station and hence the energy consumption is reduced.

$$W_i = \left\lceil A_i/H \right\rceil \quad (5.1)$$

$$H_i = \left\lceil A_i/W_i \right\rceil \quad (5.2)$$

Once the W_i and H_i values are determined the eOCSA will map the current burst into the DL part of the current frame using bottom to top and right to left tracing. Starting from bottom right allows enough space in the frame for the variable portion of the frame (DL-MAP) which starts on the left and has to extend towards the right. In the third part which is known as horizontal mapping the algorithm will check to see if there is any space left over the burst allocated in the second step. These spaces are known as strips. The eOCSA considers a fixed width for the strip and finds the largest allocation that can be fitted in this area. This step is repeated until it is not possible to fit any more allocations in the remaining space or no space is left. (5.4) and (5.5) show how eOCSA will find W_j and H_j for a burst to be allocated in the strips. eOCSA finds the largest A_j such that $A_j < W_i \times H_0$ where H_0 is the maximum available height in the strip which can be calculated using (5.3).

$$H_0 = H - H_i \quad (5.3)$$

$$H_j = \left\lceil \frac{A_j}{W_i} \right\rceil \quad (5.4)$$

$$W_j = \left\lceil \frac{A_j}{H_j} \right\rceil \quad (5.5)$$

Figure 5.2 depicts an example of mapping the DL bursts using the eOCSA algorithm. As can be seen from the figure for eOCSA the widths of all of these allocations (W_i, W_j, W_k, \dots) are the same (fixed) and will be determined by the width of the first allocation in each column. It has been shown that eOCSA will provide 93% allocation in each column. It has been shown that eOCSA will provide 93% throughput compared to the full search algorithm [3].

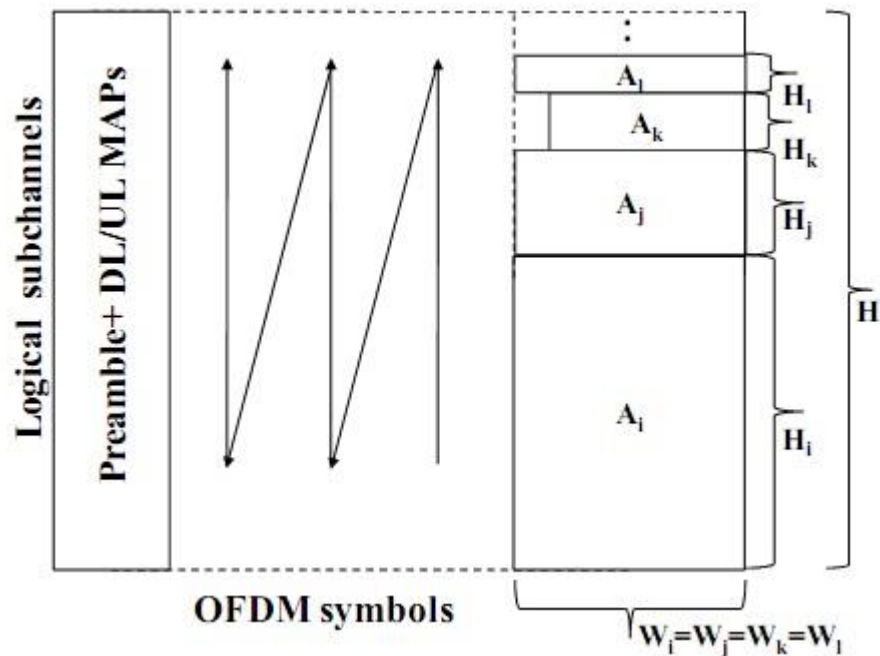


Figure 5.2: Example of Frame Packed Using eOCSA [3]

5.3 Orientation Based Burst Packing (OBBP)

The principle of the OBBP algorithm is to group up the bursts based on their orientation factors (OF) and pack the bursts of each group column-wise or row-wise into the DL sub-frame. Dealing with groups instead of independent single bursts is expected to minimize the complexity and bring an improvement in the packing efficiency also. The OBBP algorithm can be broken down into three main stages. In the first stage bursts are prepared and classified. Then the second stage makes use of the Orientation Factors (OF) for packing the bursts. Finally in the third stage the remaining bursts from previous stage are packed using the conventional best fit (BF) algorithm. For the interested reader detailed descriptions of the OBBP algorithm has been provided in [4].

5.4 Versions of the Proposed Algorithm

In this work two novel packing algorithms which have extended the classic eOCSA packing algorithm were proposed. First version of the proposed algorithm which we also refer to as the “Extended eOCSA” tries to allocate the unallocated bursts in the current frame (Leftover Bursts) into the future frames. Recalling that one frame in “Mobile WiMAX” is 5ms and the inter arrival time for G.711 packets is around 20ms this implies that it may be possible to place the left over bursts in the next 3-4 frames. The second version of the proposed algorithm introduces the concept of priority for requests in order to support the QoS requirements of different users in an OFDMA system.

5.4.1 Extended eOCSA with Regular Plus the Leftover Bursts

This algorithm simply tries to over feed the packing mechanism and tries to utilize the unused slots in future frames for packing more bursts as time goes on. It has been shown in [17] that this small variation on the eOCSA will not only help reduce the number of unused slots in a single frame but it will also help improve the overall percentage for unallocated burst in the system.

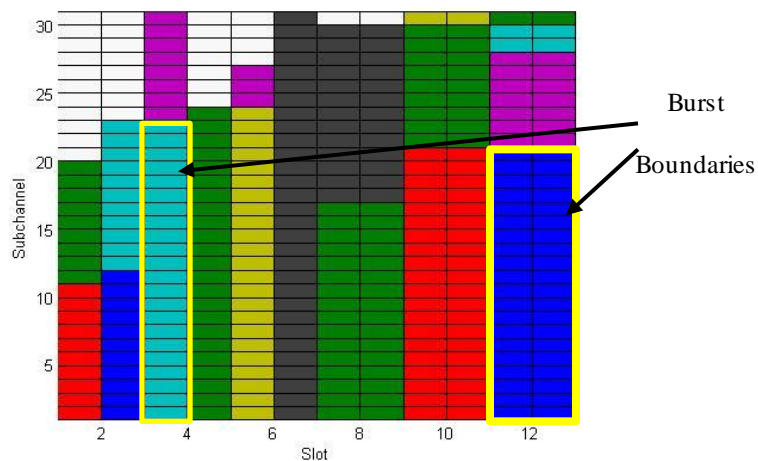
5.4.2 Priority-Aware Extended eOCSA

The second version of the proposed algorithm provides a priority-aware packing mechanism where the leftover bursts are progressively given higher priority numbers in upcoming frames. This is important since in QoS-aware networks, service-level agreements and latency constraints constitute the most important factors for scheduling real-time traffic. In this algorithm the packing mechanism tries to support the QoS-requirements of different users by assigning priorities. The algorithm assumes two classes of priorities, and assigns a priority number between 1 and 6 to each user. When the number is 1 or 2 the burst is considered as low priority and when the number is 3 to 6 the burst is assumed to be high priority. The algorithm first packs the burst in the high priority class using eOCSA and then goes to the lower priority class and tries to pack them also.

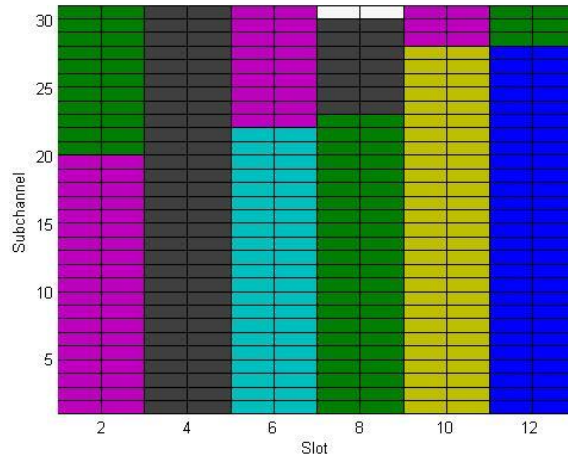
The priority number of each burst will be increased by one unit in each frame in order to update the priority number of bursts. If the priority number of a certain burst becomes larger than 6 the packing mechanism will drop that burst [17]. By assigning appropriate priority numbers to each service class of “Mobile WiMAX” or

considering latency requirements for each user this algorithm can supports QoS requirements for users.

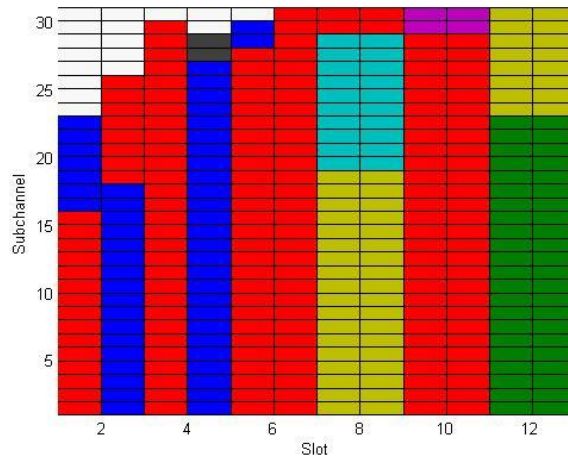
Figure 5.3 shows examples for the downlink part of the “Mobile WiMAX” frame packed using Priority-Aware Extended eOCSA. In the figure the horizontal axis shows the slots and the vertical axis denotes the sub-channels. With partially used sub-channelization, 10MHz channel and a DL/UL ratio of 29:18 (assuming 1 symbol for TTG and RTG) the DL part of the frame will have 29 symbols vs. 30 sub-channels. In this work the first 5 symbols have been used for the control information (Preamble, FCH, DL-MAP and UL-MAP) and the remaining 12 columns has been used to pack the requests of different users. Taking one symbol period for the preamble and four for the DL and UL maps leaves $12 \times 30 = 360$ slots to use for packing requests by different users. In Figure 5.3 each burst belongs to one user and unused slots have been indicated by white color.



(a)



(b)



(c)

Figure 5.3: Examples of Downlink Part of the Frame Packed With Proposed Algorithm

Chapter 6

PERFORMANCE ANALYSIS FOR PACKING

ALGORITHMS

In this section, simulation results and performance analysis of three frame packing algorithm for IEEE 802.16e “Mobile WiMAX” has been shown. Performance of the eOCSA, Extended eOCSA and Priority Aware Extended eOCSA algorithms have been evaluated using the MATLAB platform and writing dedicated functions for the different tasks. In all simulations the channel model was assumed to be the COST-231 Hata model where user’s distance from base station has been uniformly distributed and each user has speed uniformly distributed ranging from 0 to 60 km/h either toward or away from the base station. Throughout the simulations it was also assumed that the admission control mechanism has only admitted 20 users. Figure 6.1 and Figure 6.2 below show the distribution of users in the macro cell environment based on the separation between the MS and the BS for two different occasions.

Throughout simulations Variable Bit Rate (VBR) traffic was assumed for each user. To start with, each user that had been admitted by the call admission mechanism was assumed to have a traffic load that is in the range 0-260 bytes per frame (chosen from a uniform distribution). Also, to test the algorithms under extra load the second set of simulations assumed that the maximum bytes that each user can send per frame were increased to 312 bytes (20% load increase). For each run 1200 frames

corresponding to 6 seconds worth of simulation time was assumed. Each algorithm has been evaluated 100 times and the results have been averaged to give the average percentage of unallocated bursts.

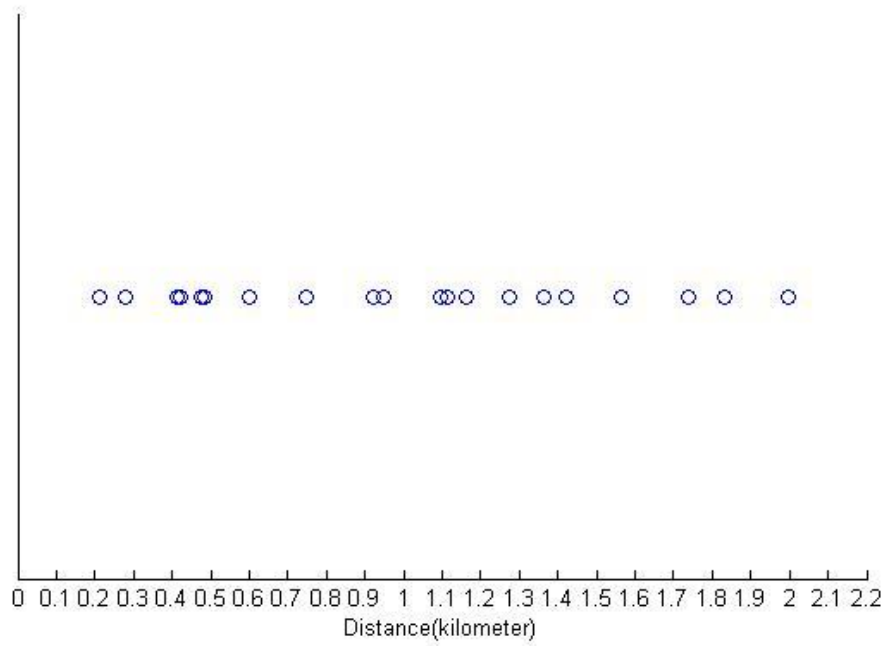


Figure 6.1: Distance of MS From Base Station in Occasion1

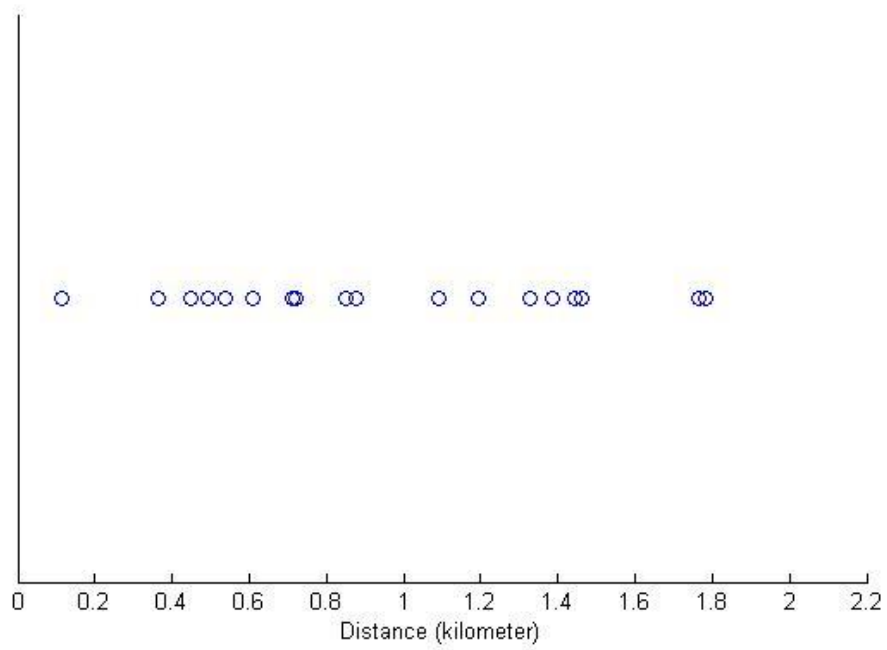


Figure 6.2: Distance of MS From Base Station in Occasion2

Figure 6.3 and Figure 6.4 below show the locations for two different mobile stations during one instance of the 100 runs. As mentioned before, users were assumed to move either away or toward the base station with equal probability.

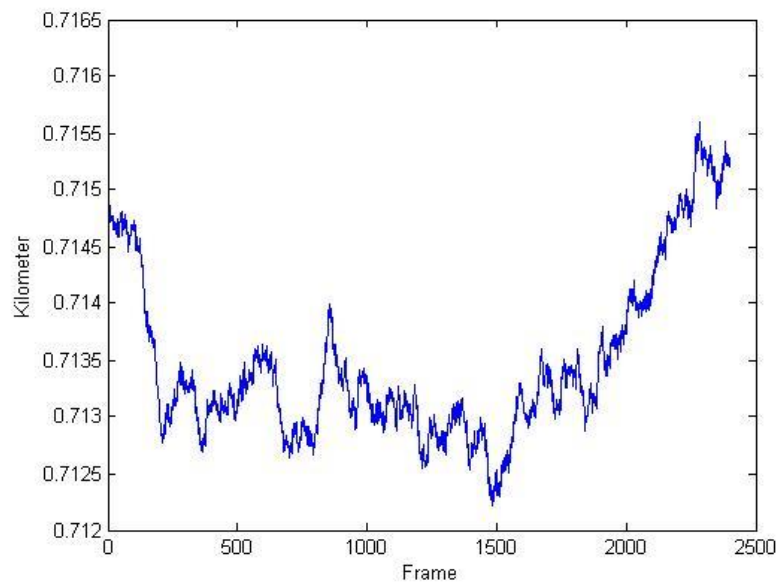


Figure 6.3: Location of MS #1 During One Simulation Run

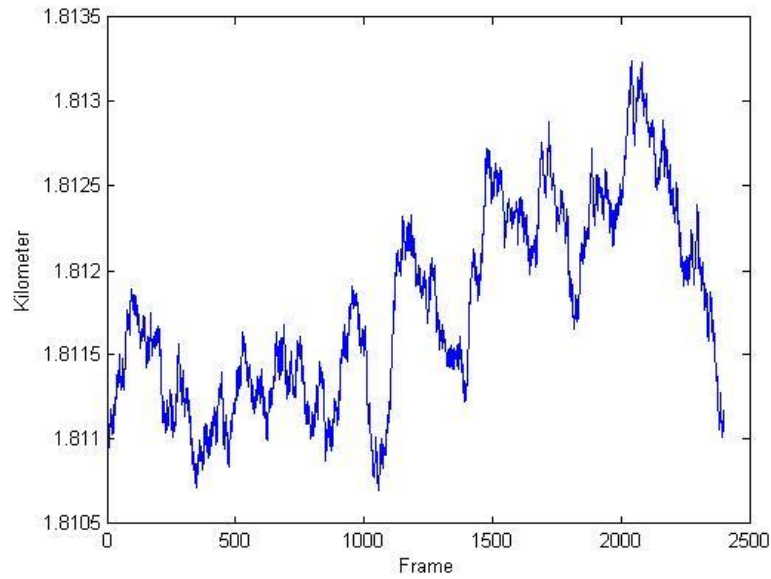


Figure 6.4: Location of MS #2 During The Same Simulation Run as in Fig. 6.3

In “Mobile WiMAX” the signal to noise ratio (SNR) of each user will be evaluated in each frame period prior to packing burst into the current frame. Figure 6.5 depicts the distance of admitted users (20 in total) from the base station for one frame. For the same frame, Figure 6.6 and Figure 6.7 respectively show the path loss and the SNR of each user in the frame.

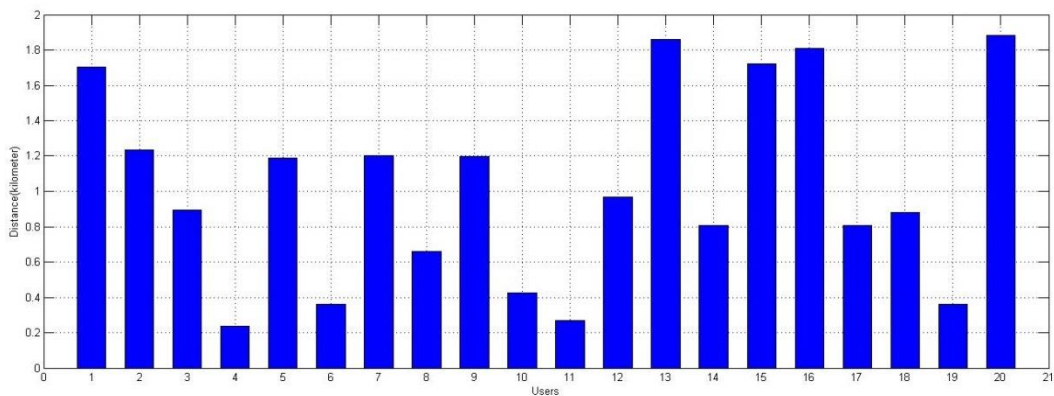


Figure 6.5: Distance of Users From Base Station

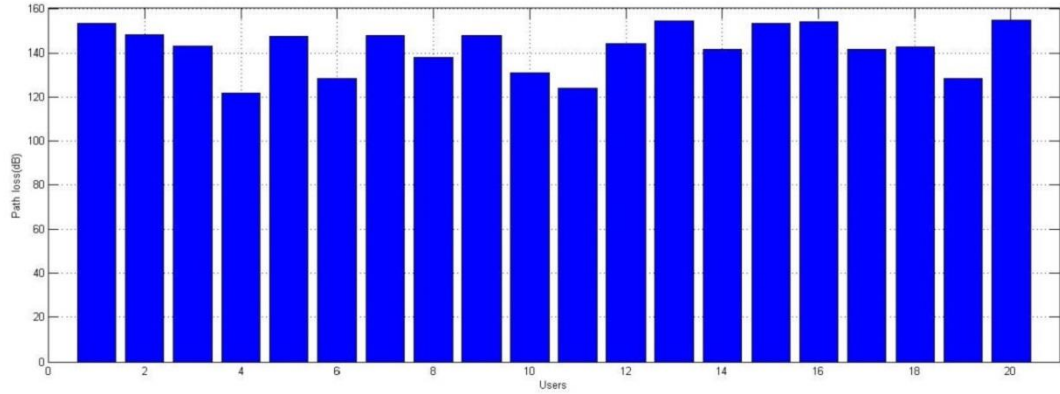


Figure 6.6: Path Loss for Individual Users in The Frame

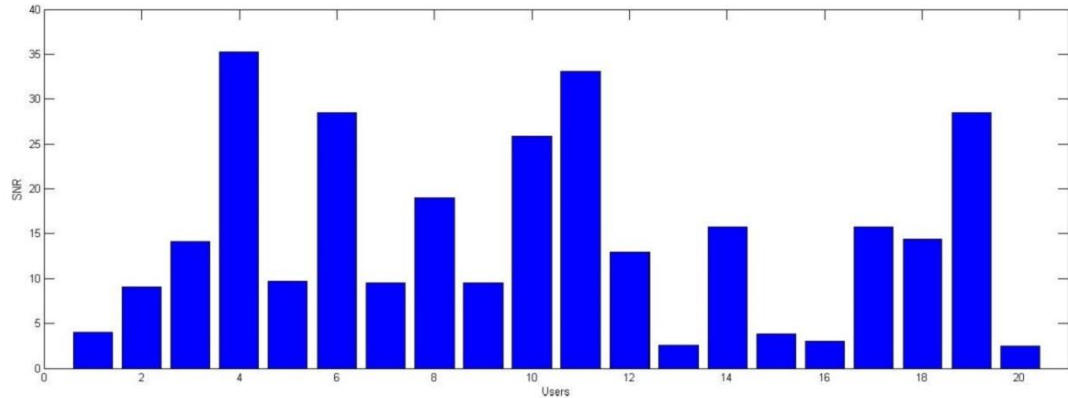


Figure 6.7: SNR of Each User in The Frame

In what follows we first compare the performance of the eOCSA packing algorithm with that of the proposed extended eOCSA algorithm that handles the regular bursts together with those that were not fitted in previous frames. Afterwards the priority aware version of the extended eOCSA is compared with the standard eOCSA. The comparisons are based on the average percentage of unallocated bursts.

The performance of eOCSA and Extended eOCSA has been evaluated for twenty users with VBR traffic drawn from a uniform distribution in the range 0 to 260 bytes

per frame (normal traffic load). The Priority-Aware Extended eOCSA algorithm that uses two classes of priorities was simulated assuming both normal traffic load and 20 percent increased traffic load. For simulations dealing with Priority-Aware Extended eOCSA, 75% of the users were considered as low priority and the remaining 25% were accepted to be in the high priority class. Figure 6.8 and Figure 6.9 respectively show examples of 5ms frames packed using the eOCSA and the proposed extended eOCSA algorithms. As mentioned before in these figures white slots correspond to unused slots and each burst (rectangles with different colors) belongs to one user.

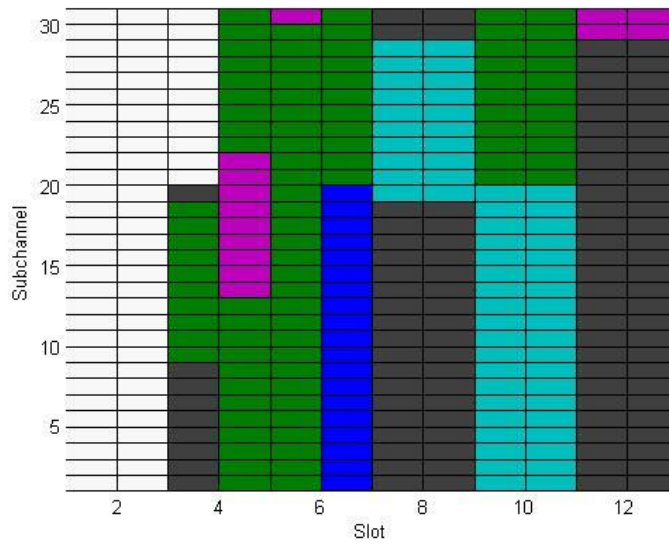


Figure 6.8: Frame Packed Using eOCSA

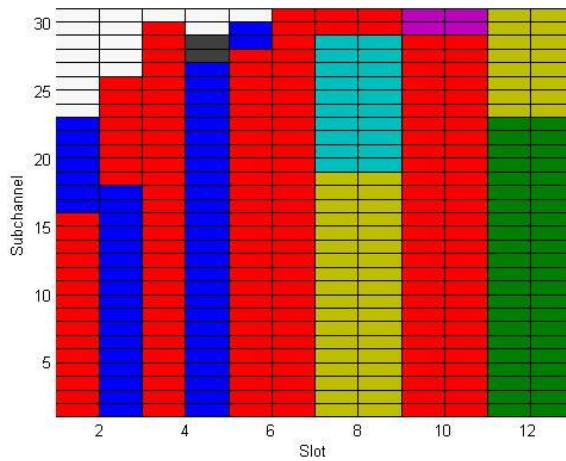


Figure 6.9: Frame Packed Using Extended eOCSA

Figures 6.10 and 6.11 provide the percentage of unallocated burst for 100 trials under normal load using eOCSA and Extended eOCSA respectively. Each trial had assumed 1200 frames.

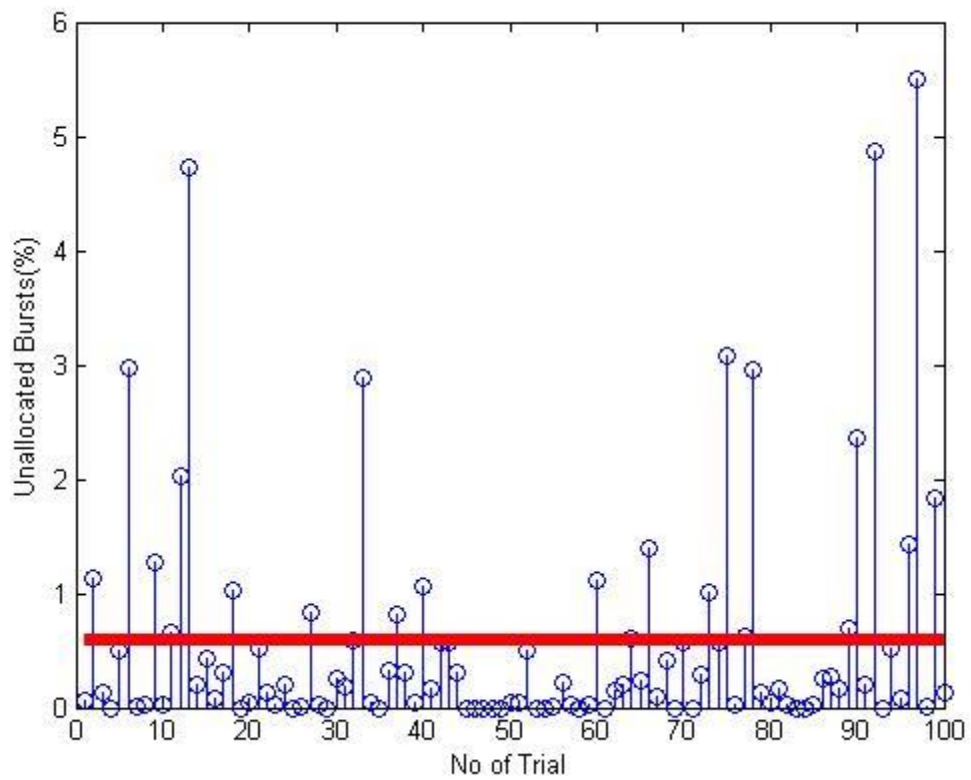


Figure 6.10: Percentage of Unallocated Bursts for eOCSA in 100 Trials

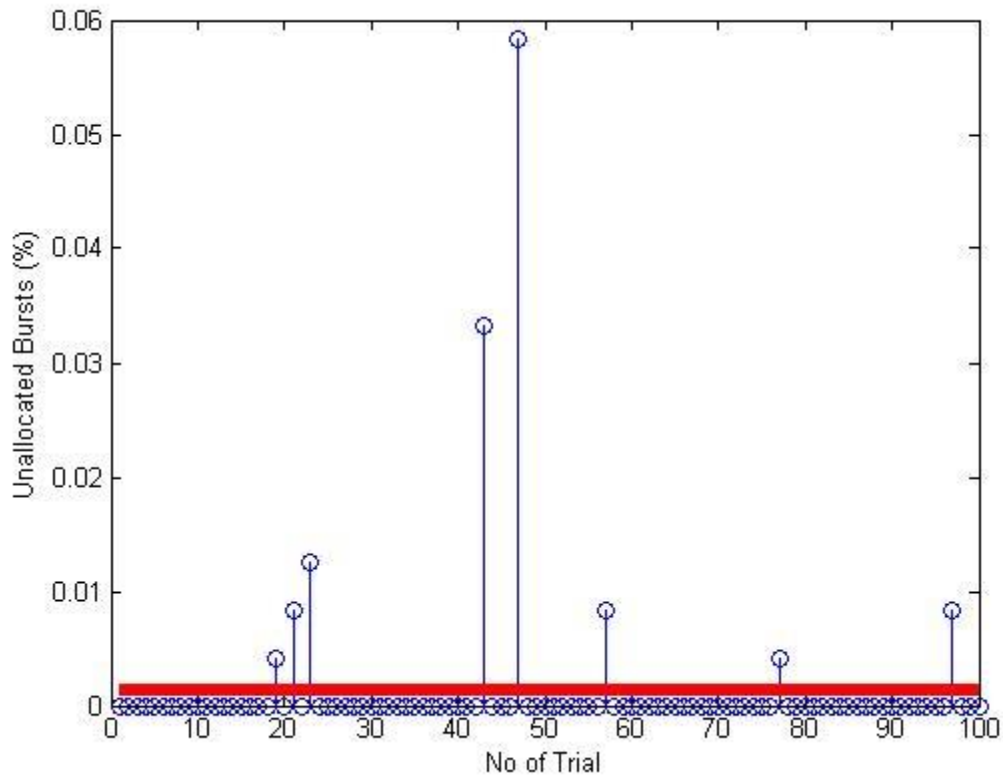


Figure 6.11: Percentage of Unallocated Bursts Using Extended eOCSA for 100 Trials

Figure 6.10 and Figure 6.11 show the percentage of unallocated bursts for each trial when eOCSA and Extended eOCSA algorithms are used for placing bursts into frames. The mean and the standard error for average percentage of unallocated bursts are 0.584 and 0.105% for the eOCSA and 0.0014 and 0.00069 for the Extended eOCSA. Results obtained using the Priority-Aware Extended eOCSA has been plotted in Figure 6.12 and the mean and standard error for the average percentage of unallocated bursts is 0.0048 and 0.0021 respectively.

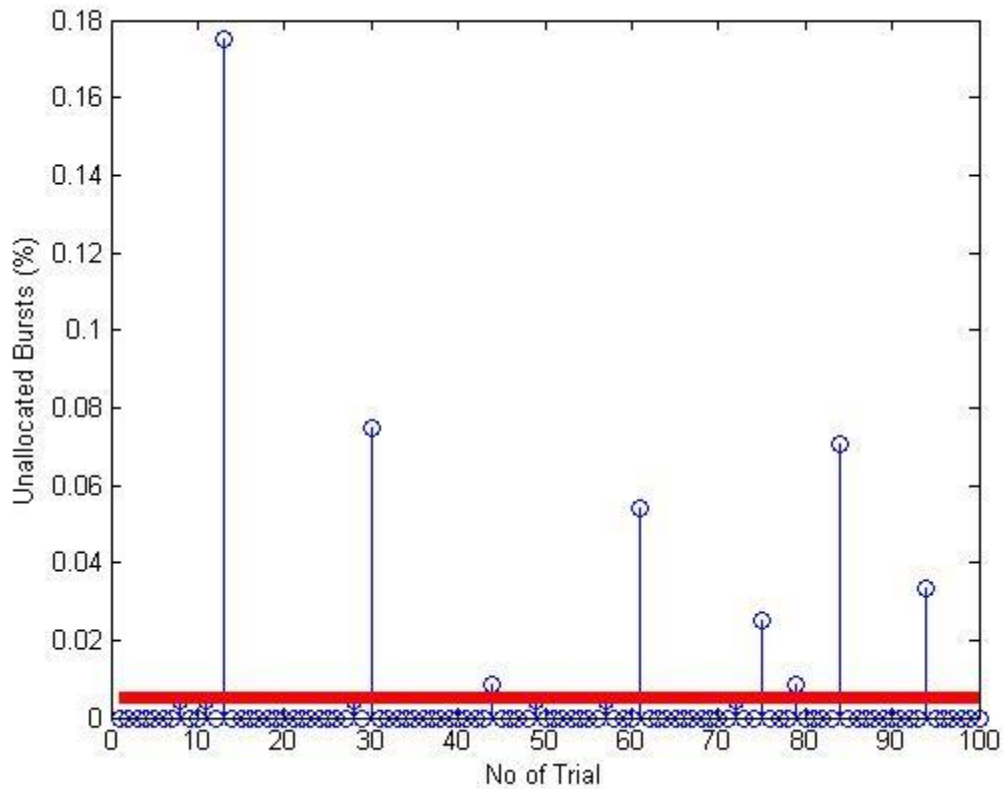


Figure 6.12: Percentage of Unallocated Bursts Using Priority-Aware Extended eOCSA Under Normal Load for 100 Trials

Figure 6.13 shows the percentage of unallocated bursts for Priority-Aware Extended eOCSA algorithm with 20% increase in load over 100 trials. It is clear from the results that even with 20% increased traffic load the Priority-Aware Extended eOCSA algorithm can still perform acceptably well. In this case the mean percentage and standard error of unallocated bursts are 3.32 and 0.75 respectively. Any value below 5% indicates the packing algorithm's efficiency in using the rectangular space in the DL part of the frame so that as few bursts as possible are left unallocated. Figure 6.14 shows the percentage of unallocated burst using eOCSA packing algorithm under 20% extra load and the mean and standard error for the average percentage of unallocated bursts is 5.36 and 0.54 respectively.

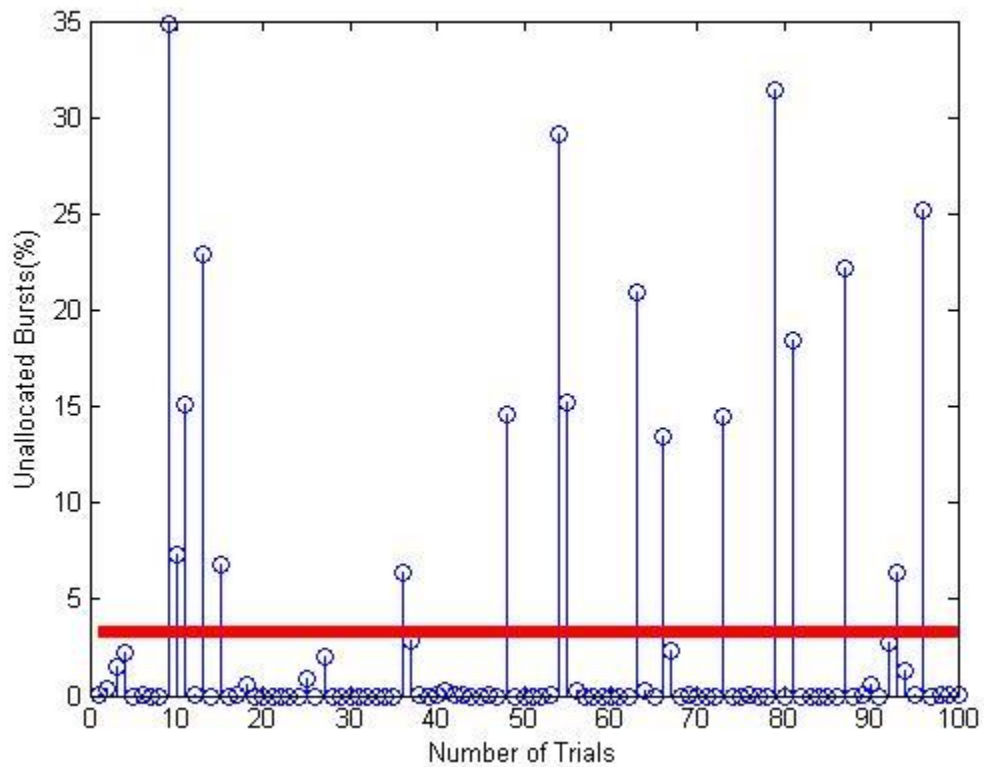


Figure 6.13: Percentage of Unallocated Bursts Using Priority Aware Extended eOCSA Under 20% Extra Load for 100 Trials

Comparing obtained values for percentage of unallocated bursts regarding three aforementioned algorithms (eOCSA, Extended eOCSA and Priority-Aware Extended eOCSA) it can be confirmed that the two proposed algorithms (Extended eOCSA and Priority Aware Extended eOCSA) can perform much better than eOCSA in a VBR traffic scenario.

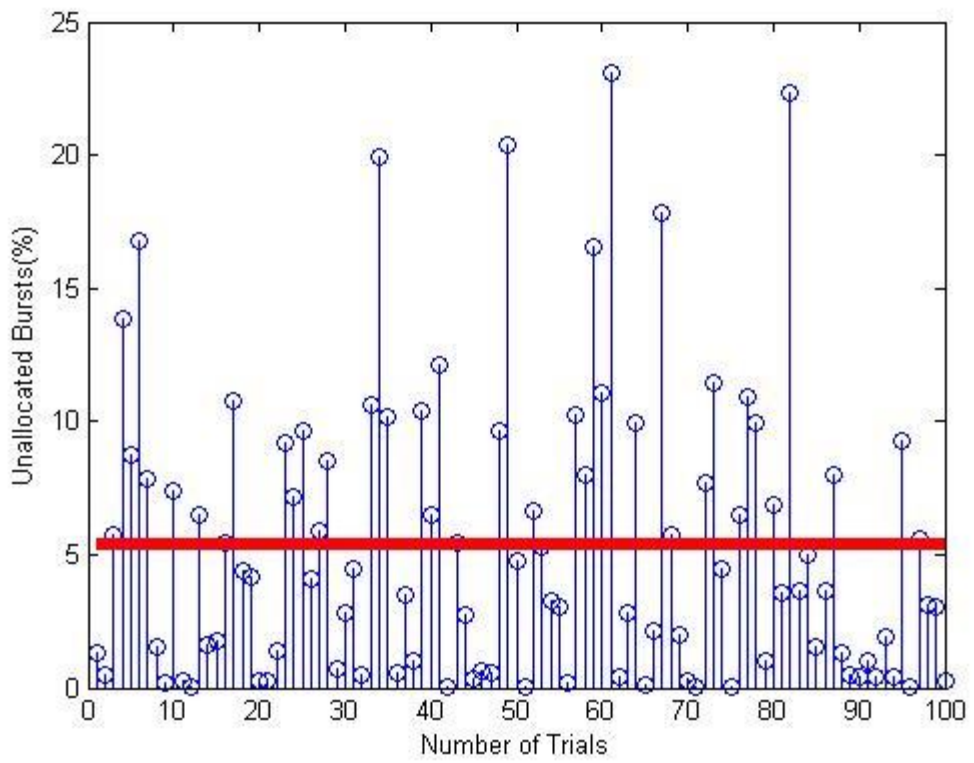


Figure 6.14 : Percentage of Unallocated Bursts Using eOCSA Under 20% Extra Load for 100 Trials

Chapter 7

CONCLUSIONS AND FUTURE WORK

7.1 Conclusions

In this work a novel algorithm with two extensions to the eOCSA algorithm has been proposed. The first extension simply tries to accommodate bursts that cannot be fitted in their frames in future frames and the second extension provides a priority-aware packing mechanism where the leftover bursts are progressively given higher priority numbers in upcoming frames.

Performance of the two proposed algorithms and the standard eOCSA packing algorithm has been evaluated in an urban region assuming a macro-cell environment of radius 2000 meters and the COST231 HATA channel model. With 20 admitted users and VBR traffic with a maximum of 260 bytes per frame the results indicate that each of the two proposed algorithms can outperform the eOCSA packing algorithm. The performance of the Priority-Aware Extended eOCSA packing algorithm is particularly good since it can keep the mean percentage of unallocated bursts around 3% even under 20% traffic load increase.

7.2 Future Work

In the future, the first piece of work that needs to be completed would be to compute the absolute carrier indices of sub-channels used by each burst placed in a frame (Using the PUSC GUI introduced in Chapter 3). Then the data for different users will be transmitted over the COST231 HATA channel and the throughput for the Priority-Aware Extended eOCSA packing algorithm would be computed.

The author could also test the proposed Priority-Aware Extended eOCSA packing algorithm under different traffic models. For example Autoregressive (AR) Models are known to be suitable for simulating the output bit rate of a VBR video source. Using 2-AR processes as suggested by Corte [29] are known to lead to models that could fit the experimental data more properly than a single AR process.

Finally, since 4th Generation Mobile Wireless Networks are evolving around MIMO-OFDM multiple access systems the future work should consider combining transmit and receive diversity schemes such as 2×1 or 2×2 Alamouti STBCs with OFDMA.

REFERENCES

- [1] Chakchai So-In, Raj Jain, Abdel-Karim Al Tamimi, "Scheduling in IEEE 802.16e Mobile WiMax Networks:Key Issues and a Survey," *IEEE journal on Selected Areas in Communication*, vol. 27, no. 2, pp. 156-170, 2009.

- [2] Ahmed M. Husein Shabani, M. T. Beg, Ammar Abdul-Hamed Khader, "Survey of Down Link Data Allocation Algorithms in IEEE 802.16 WiMAX," *International Journal of Distributed and Parallel Systems (IJDPS)*, vol. 3, no. 4, pp. 196-207, July 2012.

- [3] Chakchai So-In, Raj Jain, Abdel-Karim Al Tamimi, "eOCSA: An Algorithm for Burst Mapping with Strict QoS Requirements in IEEE 802.16e Mobile WiMAX Networks," in *2nd IFIP Wireless Days (WD)*, pp. 1-5 ,15-17 Dec. 2009.

- [4] Omar M. Eshanta, M. Ismail, and Kasmiran Jumari, "OB BP: An Efficient Burst Packing Algorithm for IEEE 802.16e Systems," *ISRN Communications and Networking*, pp. 1-5 , 2011.

- [5] R. W. Chang, "Synthesis of band-limited orthogonal signals for multi-channel data transmission," *Bell System Technical Journal*, vol. 45, no. 10, pp. 1775-1796, 1966.

- [6] S. B. Weinstein and P. M. Ebert, "Data transmission by frequency-division multiplexing using Discrete Fourier Transform," *IEEE Transactions on Communication*, vol. 19, no. 5, pp. 628-634, Oct 1971.
- [7] A. Peled, A. Ruiz, "Frequency domain data transmission using reduced computational complexity algorithms," in *IEEE International conference of Acoustics, speech and signal processing (ICASSP)*, Denver, 1980, pp. 964-967.
- [8] W. E. Keasler, D. L. Bitzer and P. T. Tuckerr, "High-speed modem suitable for operating with a switched network". *Patent 4 206 320*, 3 Jun 1980.
- [9] L. J. Cimini, "Analysis and simulation of a digital mobile channel using orthogonal frequency division multiplexing," *IEEE Transactions on Communication*, vol. 33, no. 7, pp. 665-675, 1985.
- [10] Ming Jiang, Lajos Hanzo, "Multiuser MIMO-OFDM for Next-Generation Wireless Systems," *Proceedings of IEEE*, vol. 95, no. 7, pp. 1430-1469, 2007.
- [11] IEEE Std 802.16™, "IEEE Standard for local and metropolitan area networks, Part 16: Air Interface for Fixed and Mobile Broadband Wireless Access systems, Amendment 2," May 2005.
- [12] Y. Ben-Shimol, I. Kitroser, Y. Dinitz, "Two-dimensional mapping for wireless OFDMA systems," *IEEE Transactions on Broadcasting*, vol. 52, no. 3, pp. 388-

396, 2006.

- [13] Xin Jin, Jihua Zhou, Jinlong Hu, Jinglin Shi, Yi Sun, and Eryk Dutkiewicz, "An Efficient Downlink Data Mapping Algorithm for IEEE802.16e OFDMA Systems," in *IEEE GLOBECOM*, 2008, pp. 1-5.
- [14] Ting Wang, Hui Feng, Bo Hu, "Two-dimensional resource allocation for OFDMA system," in *International Conference on Communications Workshops*, May 2008, pp. 1-5.
- [15] Marc C. Necker, Martin Kohn, Andreas Reifert, Joachim Scharf, Jorg Sommer, "Optimized Frame Packing for OFDMA Systems," in *IEEE Vehicular Technology Conference*, 2008, pp. 1483- 1488.
- [16] Chakchai So-In, Raj Jain, Abdel-Karim Al Tamimi, "OCSA: An algorithm for Burst Mapping in IEEE 802.16e Mobile WiMAX Networks," in , *Proceedings 15th Asia-Pacific Conference on Communications (APCC 2009)*, Sanghai China, 8th-10th Oct 2009, pp. 55-58.
- [17] Keivan Bahmani, Erhan. A. Ince, and Dogu Arifler, "Priority-Aware Downlink Frame Packing Algorithm for OFDMA-Based Mobile Wireless Systems," in *IEEE Signal Processing and Communications Applications Conference (SIU)*, Kyrenia, North Cyprus, 2013.
- [18] Samuel C. Yang, *OFDMA System Analysis and Design*, Artech House, 2010.

- [19] Leonhard Korowajczuk, *LTE, WiMAX and WLAN Network Design, Optimization and Performance Analysis*, Wiley, August 22, 2011.
- [20] M. Engels, *Wireless OFDM Systems: How to make them work?*, The Springer, 2002.
- [21] L. Nuaymi, *WiMAX: Technology for Broadband Wireless Access*, John Wiley & Sons, 2007.
- [22] Jamal Mountassir , Horia Balta , Marius Oltean , Maria Kovaci, Alexandru Isar, "Simulating the WiMAX Physical Layer in Rayleigh Fading Channel," *Journal of Wireless Networking and Communications*, pp. 1-24, 2011.
- [23] Masood Maqbool, Marceau Coupechoux, Philippe Godlewski, "Subcarrier permutation types in IEEE 802.16e," in *TELECOM ParisTech*, pp. 1-24, 2008.
- [24] M. Hata, "Empirical formula for propagation loss in land mobile radio services," *IEEE Transactions on Vehicular Technology*, vol. 29, pp. 317-325, 1981.
- [25] V. S. Abhayawardhana, I. J. Wassell, M. P. Sellars, M. G. Brown, "Comparison of empirical propagation path loss models for fixed wireless access systems," in *IEEE Vehicular Technology Conference*, 2005 , pp. 73-77 .
- [26] "IEEE Standard for Local and metropolitan area networks Part 16: Air Interface

for Broadband Wireless Access Systems," *IEEE*, New York, 29 May 2009.

- [27] M. Garey and D. Johnson, *Computers and Intractability: A Guide to the Theory of NP-Completeness*, W. H. Freeman, January 15, 1979.
- [28] Claude Desset, Eddie Batista, Lima Filho, "WiMAX Downlink OFDMA Burst Placement for Optimized Receiver Duty-Cycling," in *IEEE International Conference on Communications*, 2007, pp. 5149-5154 .
- [29] A. La Corte, A. Lombardo, S. Palazzo, and S. Zinna, , "Modeling activity in VBR video sources," *Signal Processing: Image Communication*, vol. 3, pp. 167-178, 1991.
- [30] Yi-Neng Lin a, Ying-Dar Lin a, Yuan-Cheng Lai b, Che-Wen Wu a, "Highest Urgency First (HUF): A latency and modulation aware bandwidth allocation algorithm for WiMAX base stations," *Computer Communications*, no. 32, pp. 332-342, 2009.
- [31] Tao Jiang, Weidong Xiang, Hsiao-Hwa Chen, Qiang Ni, "Multicast Broadcast Services Support in OFDMA-Based WiMAX Systems", *IEEE Communications Magazine, IEEE*, vol. 45, no. 8, pp. 78-86, August 2007.
- [32] Amit Kumar, Yunfei Liu, Tanvir Singh, Sawtantar Singh Khurmi, "IMT-Advanced: The ITU standard for," *International Journal of Computer Science*

and Technology, 2011.

[33] B. R. Saltzberg, "Performance of an efficient parallel data transmission system," *IEEE Transactions on Communication*, vol. 15, no. 6, pp. 805-811, December 1967.

[35] Gordon L. Stüber, *Principle of Mobile Communication*, Springer, 2011, pp. 22-24.

[36] "Physical layer aspects for evolved universal terrestrial radio access (UTRA)," 3GPP TR 25.814 V7.1.0, pp. 1–132, Sept. 2006.